Journal of Medicinal Chemistry Article

J. Med. Chem. **2009,** *52,* 7289–7300 **7289**
DOI: 10.1021/jm900915x

Discovery of Novel Benzoxazinones as Potent and Orally Active Long Chain Fatty Acid Elongase 6 Inhibitors

Takashi Mizutani,* Shiho Ishikawa, Tsuyoshi Nagase, Hidekazu Takahashi, Takashi Fujimura, Takahide Sasaki, Akira Nagumo, Ken Shimamura, Yasuhisa Miyamoto, Hidefumi Kitazawa, Maki Kanesaka, Ryo Yoshimoto, Katsumi Aragane, Shigeru Tokita, and Nagaaki Sato

Tsukuba Research Institute, Merck Research Laboratories, Banyu Pharmaceutical Co., Ltd, Okubo 3, Tsukuba, Ibaraki 300-2611, Japan

Received June 22, 2009

A series of benzoxazinones was synthesized and evaluated as novel long chain fatty acid elongase 6 (ELOVL6) inhibitors. Exploration of the SAR of the UHTS lead **1a** led to the identification of (*S*)-**1y** that possesses a unique chiral quarternary center and a pyrazole ring as critical pharmacophore elements. Compound (*S*)-**1y** showed potent and selective inhibitory activity toward human ELOVL6 while displaying potent inhibitory activity toward both mouse ELOVL3 and 6 enzymes. Compound (*S*)-**1y** showed acceptable pharmacokinetic profiles after oral dosing in mice. Furthermore, (*S*)-**1y** significantly suppressed the elongation of target fatty acids in mouse liver at 30 mg/kg oral dosing.

Introduction

The incidence of type 2 diabetes has dramatically increased over the past decade. Accumulated evidence suggests a strong correlation between insulin resistance and the development of type 2 diabetes mellitus. An increase in de novo lipid synthesis and fat storage in tissues such as liver leads to dysfunction in those tissues (i.e., insulin resistance).[1] Although it is unclear how an increased intracellular lipid content deteriorates tissue and whole body insulin sensitivity, it has been suggested that increased levels of long chain fatty acyl-CoAs antagonize the metabolic actions of insulin.[2] Interestingly, recent reports suggested that alternation of the specific fatty acid component (i.e., palmitoleate) has a significant impact on the insulin sensitivity of the liver and the whole body.[3,4]

With regard to de novo lipid synthesis, microsomal enzymes are responsible for the elongation of long chain fatty acyl-CoA with chain lengths over C16, while fatty acid syntheses in the cytosol are responsible for the de novo synthesis of the fatty acyl-CoAs with chain lengths up to C16.[5,6] Fatty acyl-CoA elongation at microsomal fractions requires four sequential steps: (1) condensation between fatty acyl-CoA and malonyl-CoA to generate β-ketoacyl-CoA by ELOVL[a] (long chain fatty acid elongase); (2) reduction by β-ketoacyl-CoA reductase; (3) dehydrogenation by β-hydroxyacyl-CoA dehydrogenase; (4) reduction by *trans*-2,3-enoyl-CoA reductase.[5,6] ELOVL family enzymes are responsible for the rate-limiting and initial condensation reaction.[7,8]

So far, seven ELOVL enzymes have been identified in mammals and are designated ELOVL1−7.[7−12] Each ELOVL enzyme exhibits different fatty acyl-CoA substrate preferences and different tissue distributions, suggesting that they play distinct physiological roles in vivo.[13] Among ELOVL family members, ELOVL6 (known as LCE, FACE) shows the highest amino acid sequence homology to ELOVL3 in humans and mice (46% and 44%, respectively).[14a] Not surprisingly, ELOVL3 and ELOVL6 show overlapped substrate specificity: ELOVL6 regulates the elongation of saturated and monosaturated fatty acyl-CoAs with C12−16,[5−8] whereas ELOVL3 regulates the synthesis of saturated and monounsaturated fatty acyl-CoAs with more broad range of chain length including very long chain fatty acyl-CoAs with C16−C24.[15]

While ELOVL3 and ELOVL6 display unique respective expression patterns, they both are expressed in highly lipogenic tissues such as liver and adipose. Regarding the regulatory mechanism for expression, liver ELOVL6 expression is up-regulated by feeding after fasting, high carbohydrate diet, and obesity in rodents, suggesting that ELOVL6 expression is controlled by energy balance and nutrient inputs.[7,8,16] In contrast, liver ELOVL3 expression is under circadian control: ELOVL3 shows high expressions in the inactive phase and low expressions in the active phase.[17] Given their primary roles in the elongation of long chain fatty acyl-CoAs (e.g., palmitoyl-CoA) and expressions in lipogenic tissues, ELOVL3 and ELOVL6 are considered to play important physiological roles in the lipid metabolism. In fact, ELOVL6 regulates hepatic insulin sensitivity by modulating the fatty acid components,[4] while ELOVL3 plays important roles in the regulation of triglyceride formation in skin and brown adipose tissue and regulates thermogenesis.[15,21] Although the increasing information regarding the physiological and pathological roles of ELOVLs garnered much attention from research scientists, lack of chemical tools precluded their ability to further address

*Phone: 81-29-877-2000. FAX: 81-29-877-2029. Email: miztnitk@gmail.com.

[a] Abbreviations: ELOVL, long chain fatty acid elongase; SAR, structure−activity relationship; hELOVL, long chain fatty acid elongase in human; mELOVL, long chain fatty acid elongase in mice; UHTS, ultra-high-throughput screening; PMB, *p*-methoxybenzyl; CAN, cerium ammonium nitrate; SD rat, Sprague−Dawley rat; LDA, lithium diisopropylamide; EDCI, 1-ethyl-3-(3-dimethylaminopropyl)carbodiimide; HOBt, 1-hydroxybenzotriazole.

Published on Web 11/02/2009

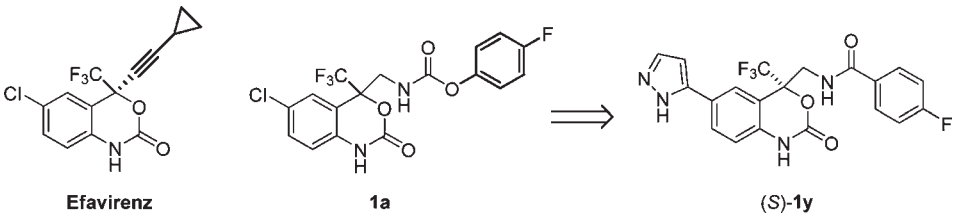

Figure 1

Scheme 1[a]

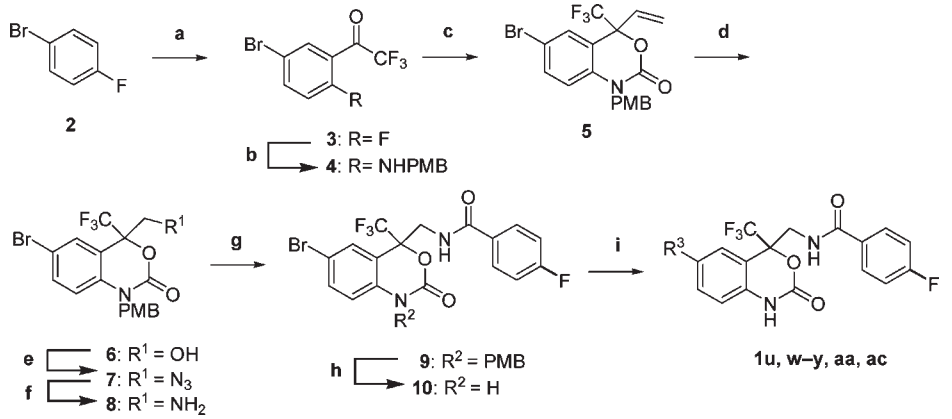

[a] Reagents and conditions: (a) LDA, THF, −40 °C, 1 h; ethyl trifluoroacetate, −78 °C, 1 h, 62%; (b) 4-methoxybenzylamine, K_2CO_3, toluene, reflux, 12 h, 83%; (c) (i) vinylmagnesium bromide, THF, 0 °C, 1 h; (ii) triphosgene, triethylamine, toluene, 0 °C, 30 min, 83% in 2 steps; (d) O_3, CH_2Cl_2, MeOH, −78 °C, 2 h; then $NaBH_4$, 0 °C, 10 min, 87%; (e) (i) Tf_2O, 2,6-lutidine, $CHCl_3$, THF, 0 °C, 1 h; (ii) NaN_3, DMF, 80 °C, 3 h, 71% in 2 steps; (f) (i) trimethylphosphite, THF, H_2O, 60 °C, 12 h; (ii) 4 N HCl in dioxane, rt, 24 h, 71% in 2 steps; (g) 4-fluorobenzoic acid, EDCI·HCl, HOBt·H_2O, TEA, DMF, 0 °C, 12 h, 90%; (h) CAN, CH_3CN, H_2O, rt, 4 h, 90%; (i) cross coupling with aryl boronic acids or aryl zinc reagents.

the pharmacological roles of ELOVLs and their therapeutic potentials.

In order to identify chemical tools for ELOVL enzyme studies, we recently established a homogeneous enzyme assay for ELOVL6, which is applicable to UHTS using the recombinant histidine-tagged acyl-CoA binding protein as a molecular probe for the detection of radioactive products of ELOVL6.[22] The UHTS of our corporate sample collections resulted in the discovery of a benzoxazinone class of lead **1a** (Figure 1). Importantly, **1a** shares the core benzoxazinone structure with Efavirenz, a commercial non-nucleoside HIV-1 reverse transcriptase inhibitor, suggesting druggability of the structure of **1a**.[23]

We have recently reported the discovery of two structurally diverse indoledione and 3-sulfonyl-8-azabicyclo[3.2.1]octane derivatives as ELOVL6 selective inhibitors.[14b,c] In this report, we describe the discovery of a structurally divergent benzoxazinone class of ELOVL6 inhibitors. The advanced derivative (*S*)-**1y** (Figure 1) was found to possess potent and selective inhibitory activity toward human ELOVL6 and potent dual inhibitory activity toward mouse ELOVL3 and ELOVL6. The in vitro selectivity and in vivo profiling of (*S*)-**1y** is also reported.

Chemistry

The general synthetic route for compounds **1** is shown in Schemes 1 and 2. 4-Bromofluorobenzene (**2**) was selectively deprotonated with LDA, followed by trifluoroacetylation to give trifluoroacetophenone **3**. The activated fluorine atom of **3** was substituted with *p*-methoxybenzylamine to give **4**. Vinylation of **4**, followed by cyclization in the presence of triphosgene, gave the benzoxazinone core **5**. Ozonolysis of the vinyl group of **5** and reductive workup of the resultant ozonide gave alcohol **6**. Alcohol **6** was converted to the corresponding amine **8** via azide **7**. Condensation of the amine **8** with 4-fluorobenzoic acid followed by deprotection of the PMB group afforded **10**. A series of the amide derivatives were synthesized in a similar manner. Cross coupling of compound **10** with appropriate boronic acids or aryl zinc reagents furnished a variety of 6-substituted derivatives (Scheme 1). Alternatively, the bromide **9** was converted to the corresponding iodide **11**, which was treated with various nitrogen nucleophiles to furnish the target compounds after cleavage of the PMB group (Scheme 2). Optical resolution of the representative potent compound **1** and synthetic intermediate **10** was conducted to identify and evaluate active isomers by using chiral stationary HPLC.

Scheme 2[a]

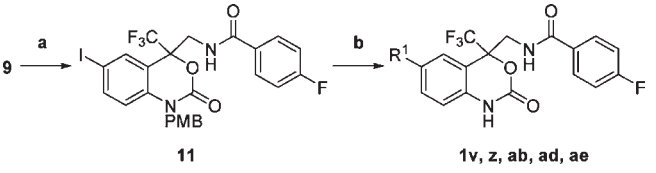

[a] Reagents and conditions: (a) CuI, NaI, *N,N'*-dimethylethylenediamine, 1,4-dioxane, 110 °C, 4.5 h, 78%; (b) (i) nitrogen nucleophiles, CuI, K_3PO_4, *N,N'*-dimethylethylenediamine, DMF, 110 °C, 1 h; (ii) $AlCl_3$, anisole, 100 °C, 2 h.

Results and Discussion

Structure−Activity Relationships. SAR exploration of the benzoxazinone lead **1a** began with replacement of the

Table 1. SAR on the Substituents on the Quarternary Carbon **1a**−**f**[a]

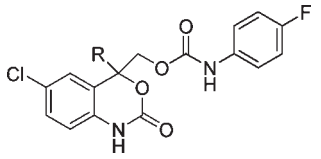

compound	R	hELOVL6 IC_{50} (nM)
1a	CF_3	142 ± 16[b]
1b	Me	1364[c]
1c	Et	2255[c]
1d	*i*-Pr	5031[c]
1e	cyclopropyl	1414[c]
1f	Ph	> 10 000[c]

[a] Inhibitory activity of compounds on human ELOVL6 for palmitoyl-CoA elongation. [b] The values represent the mean ± SE for $n \geq 3$. [c] The values are means of two independent experiments.

Table 2. SAR on the Side Chain Unit **1a** and **1g**−**i**[a]

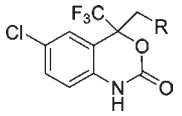

compound	R	hELOVL6 IC_{50} (nM)
1a	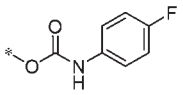	142 ± 16
1g	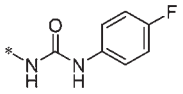	33 ± 2
1h	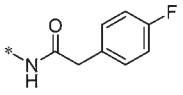	646 ± 28
1i	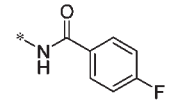	26 ± 2

[a] Inhibitory activity of compounds on human ELOVL6 for palmitoyl-CoA elongation. The values represent the mean ± SE for $n \geq 3$.

trifluoromethyl group at the unique quaternary center. Replacement of the trifluoromethyl group with methyl (**1b**), ethyl (**1c**), isopropyl (**1d**), cyclopropyl (**1e**), and phenyl (**1f**) resulted in a significant loss of potency, demonstrating that the unique trifluoromethyl-substituted quaternary center is essential for ELOVL6 inhibitory activity (Table 1). Hence, we focused our efforts on optimization of the side chain unit and substituents on the benzoxazinone core.

The SAR for the right-hand linkage unit was examined initially (Table 2), because the carbamate linkage of **1a** was found to be metabolically labile (extensive hydrolysis after incubation with microsomes, data not shown). Replacement of the oxygen atom on the side chain of **1a**, conserving the bond length, led to the identification of the urea derivative **1g** with a 4-fold enhancement in activity. On the other hand, the corresponding phenyl acetamide derivative **1h** exhibited a decrease in activity. Contraction by one carbon resulted in the simple benzamide derivative **1i**, which showed the most

Table 3. SAR on the Right-Hand Phenyl Moiety (**1i**−**s**) and Left-Hand 6-Substitution (**1t**−**ae**)[a]

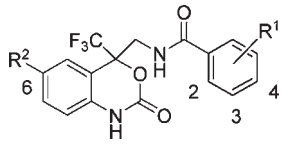

compound	R^1	R^2	hELOVL6 IC_{50} (nM)
1i	4-F	Cl	26 ± 2
1j	3-F	Cl	261 ± 20
1k	2-F	Cl	539 ± 41
1l	4-Me	Cl	38 ± 2
1m	3-Me	Cl	437 ± 89
1n	2-Me	Cl	971 ± 405
1o	4-MeO	Cl	558 ± 120
1p	4-CF_3	Cl	813 ± 362
1q	4-*i*-Pr	Cl	1869 ± 57
1r	4-Ph	Cl	> 10 000
1s	4-Ms	Cl	> 10 000
1t	4-F	H	95 ± 39
1u	4-F	Ph	1479 ± 107
1v	4-F	1-(2-pyridone)	106 ± 14
1w	4-F	4-isoxazol	121 ± 47
1x	4-F	4-pyrazol	22 ± 3
1y	4-F	3-pyrazol	4.0 ± 1
1z	4-F	1-pyrazol	26 ± 1
1aa	4-F	5-(1,2,4-triazol)	97 ± 9
1ab	4-F	1-(1,2,4-triazol)	572 ± 252
1ac	4-F	2-imidazol	537 ± 239
1ad	4-F	1-(2-pyrrolidone)	39 ± 4
1ae	4-F	3-(1,3-oxazolidin-2-one)	67 ± 7

[a] Inhibitory activity of compounds on human ELOVL6 for palmitoyl-CoA elongation. The values represent the mean ± SE for $n \geq 3$.

potent inhibitory activity. Importantly, the amide bond of **1i** is stable after microsomal incubation, while the urea linkage of **1g** is relatively unstable (data not shown); therefore, **1i** was selected as a benchmark compound for further optimization. Next, substituent effects on the benzamide group of **1i** were systemically investigated (**1i**−**s**, Table 3). Of the fluoro derivatives (**1i**−**k**), the 2- and 3-fluoro derivatives **1j** and **1k** showed markedly decreased potency compared to the 4-fluoro derivative **1i**. This trend was also observed in the methyl derivatives **1l**−**n**. These results clearly suggest that substitutions at the 2- and 3-positions are unfavorable. Thus, modification efforts were focused on the 4-position. A variety of para-substituted derivatives such as the methoxy (**1o**), trifluoromethyl (**1p**), isopropyl (**1q**), phenyl (**1r**), and methanesulfonyl (**1s**) derivatives displayed substantially decreased potency, indicating that bulky substituents are not tolerated at the 4-position. Next, the 6-substituent (R^2 group) on the core benzoxazinone ring was intensively modified using **1i** as a template (**1t**−**ae**, Table 3). The deschloride derivative **1t** showed a 4-fold decrease in potency compared to **1i**, and replacement of the chloride by a phenyl group as in **1u** resulted in a further decrease in potency. Interestingly, the pyridone derivative **1v** regained hELOVL6 inhibitory activity, which is as potent as the deschloride derivative **1t**. From these observations, we hypothesized that small and relatively polar substituents might be optimal for this position; hence, introduction of a line of five-membered heterocycles was examined. The 4-isooxazole derivative **1w** was found to have comparable activity to the pyridone derivative **1v**. We found that pyrazole substitution potentiates hELOVL6 inhibitory activity. The 4-pyrazole

Table 4. Human and Mouse ELOVL6 Enzyme Assay and Mouse Cellular Assay on Chiral Compounds[a]

compound	hELOVL6[b] IC_{50} (nM)	mELOVL6[b] IC_{50} (nM)	mouse hepatocyte H2.35[d] IC_{50} (nM)
(−)-**1g**	19 ± 1	31 ± 4.3	377 ± 152
(−)-**1i**	15 ± 2	26 ± 5.4	131 ± 25
(+)-**1i**	> 10 000	NT[c]	NT[c]
(+)-**1x**	10 ± 1	20 ± 4.9	50 ± 4.4
(*S*)-**1y**	2.6 ± 0.15	14 ± 1.2	3.6 ± 0.84
(+)-**1z**	13 ± 2	29 ± 4.8	58 ± 3.0

[a] The values represent the mean ± SE for $n \geq 3$. [b] Inhibitory activity of compounds on human or mouse ELOVL6 for palmitoyl-CoA elongation. [c] Not tested. [d] [^{14}C]Palmitic acid was used as a radioactive substrate. Elongation activity was monitored as the elongation index (total amount of C18 fatty acids/total amount of C16 fatty acids). See Experimental Section for details.

derivative **1x**, which has the same substitution pattern as 4-isooxazole, is equipotent to the parent **1i**. Furthermore, the regio-isomeric 3-pyrazole derivative **1y** was found to have a low nanomolar activity. The 1-pyrazole derivative **1z** was equipotent to the parent **1i**. Whereas introduction of a pyrazole ring enhanced hELOVL6 inhibitory activities, other five-membered heteroaromatics such as triazoles **1aa** and **1ab** and imidazole 1ac showed only moderate to weak inhibitory activities. Non-aromatic five-membered heterocycles were also briefly examined. The pyrrolidone (**1ad**) and oxazolidone (**1ae**) derivatives showed relatively potent hELOVL6 inhibitory activities. Next, optical resolution of the representative potent derivatives **1g**, 1i, and **1x**−**z** was conducted to identify and evaluate active isomers. Racemic compounds and synthetic intermediate **10** were resolved by using chiral stationary HPLC. In all cases, one isomer was found to be the active isomer, while its opposite isomer showed a complete loss in potency ((−)-**1i** and (+)-**1i**, respectively; Table 4). The absolute configuration of synthetic intermediate (*S*)-**10** was unequivocally assigned by X-ray crystallography analysis. The chiral intermediate (*S*)-**10** was successfully converted to (*S*)-**1y**, which has an opposite stereochemistry to Efavirenz (Figure 1).[23]

To evaluate the potential utility of the selected chiral compounds (−)-**1g**, (−)-**1i**, (+)-**1x**, (*S*)-**1y**, and (+)-**1z** as pharmacological tools in rodents, their inhibitory activities on mouse ELOVL6 and on the fatty acid elongation (i.e., elongation index) in mouse hepatocyte H2.35 cells were examined (Table 4). Human and mouse ELOVL6s display 96% identity in amino acid sequence.[8] Consistent with the high homology between species, those active isomers potently suppressed elongation activities of both hELOVL6 and mELOVL6. Encouraged by these results, we evaluated the inhibitory activities of these compounds on the cellular fatty acids elongation by using mouse hepatocyte H2.35 cells.[14a] Of the selected five compounds shown in Table 4, the 6-chloro derivatives ((−)-**1g** and (−)-**1i**) showed relatively large discrepancies in inhibitory actions between the enzyme and cellular assays: the amide derivative (−)-**1i** showed a 5-fold discrepancy and the urea (−)-**1g** displayed much larger 12-fold shift. On the contrary, a series of pyrazols ((+)-**1x**−**z**) showed greater consistency between the assays, and the most potent (*S*)-**1y** showed no discrepancy. Plasma protein binding seems to be responsible for the observed discrepancies. Compound (*S*)-**1y** with no discrepancy showed relatively high plasma unbound fraction (10.7%), whereas compound (−)-**1g** with a 12-fold shift showed substantially lower unbound fraction (0.5%) (Table 5). Compound (−)-**1i** with a 5-fold discrepancy has 5.3% plasma unbound fraction, which is in between those of (−)-**1g** and (*S*)-**1y**.

Table 5. Unbound Fraction Ratio of the Selected Active Isomers in Mouse Plasma[a]

compound	unbound fraction (%)
(−)-**1g**	0.5 ± 0.1
(−)-**1i**	5.3 ± 0.2
(*S*)-**1y**	10.7 ± 1.1

[a] The values represent the mean ± SE for $n = 3$. Plasma protein binding of drug was determined by equilibrium dialysis. See Experimental Section for details.

In Vitro and In Vivo Profiles of Compound (*S*)-1y. The most potent compound, (*S*)-**1y**, was further characterized (Table 6). Compound (*S*)-**1y** was highly selective for hELOVL6 over other human ELOVL family enzymes (hELOVL1, 2, 3, and 5: over 50-fold). However, (*S*)-**1y** was found to equipotently inhibit mELOVL3 and mELOVL6. When the amino acid sequence homology between human and mouse orthologs (e.g., hELOVLs vs mELOVLs) is examined, hELOVL3 displays relatively low homology to mELOVL3 (69%) while other hELOVL members show 88−96% homology to the corresponding mouse orthologs.[14a] Having considered that, we speculate that relatively low homology between human and mouse ELOVL3 proteins could explain species-related difference in affinity of (*S*)-**1y** to ELOVL3 enzymes (i.e., low affinity for hELOVL3 while high affinity for mELOVL3), which consequently resulted in the discovery of mouse ELOVL3/6 dual inhibitory activity. To the best of our knowledge, this is the first example of the ELOVL3/6 dual inhibitor, and (*S*)-**1y** could be a unique pharmacological tool as a potent mouse ELOVL3/6 dual inhibitor to potently suppress the biosynthesis of a variety of long chain fatty acids. Compound (*S*)-**1y** was screened by MDS Pharma Services (PanLabs) in a panel of 168 receptor, enzyme, channel, and transporter assays. No significant activity was observed ($IC_{50} > 10\ \mu M$) against any of the PanLabs assays.

In order to assess the utility of (*S*)-**1y** as a tool for in vivo studies, we further examined the in vivo profiles of (*S*)-**1y**. Compound (*S*)-**1y** showed acceptable pharmacokinetic profiles and appreciable plasma and liver exposure after oral dosing (Table 7). The plasma and liver levels at 2 h post 10 mg/kg oral administration of (*S*)-**1y** in mice were determined to be 0.66 μM and 12.5 μM, respectively, with a liver to plasma ratio of 19. These data suggest that (*S*)-**1y** efficiently reaches the liver where the target enzymes such as ELOVL3 and ELOVL6 abundantly exist. Although (*S*)-**1y** showed a relatively short half-life (1.9 h, Table 7), appreciable plasma exposure up to 8 h postdosing (0.7 μM, Table 8) allowed us to evaluate in vivo efficacy of (*S*)-**1y** in mice.

Initially, the effect of (*S*)-**1y** on the elongation index of the liver lipids in mice was assessed by using [^{14}C]palmitic acid as a radiotracer where the elongation index was defined as a ratio of [total amount of C18 fatty acids (C18:0, C18:1)] to [total amount of C16 fatty acids (C16:0, C16:1)] (Figure 2). We found that orally administered (*S*)-**1y** significantly reduces the elongation index of the mouse liver lipids even at 1 mg/kg (minimum effective dose). The plasma level 2 h after 1 mg/kg oral dosing was 0.54 μM, demonstrating potent in vivo activity of (*S*)-**1y** (Figure 2). Next, we examined the effects of (*S*)-**1y** on the elongation index of the net fatty acids in liver and plasma following subchronic

Table 6. Human ELOVL Subtype Selectivity and Mouse ELOVL3 and 6 Inhibitory Activities of (*S*)-**1y**[a]

enzyme	hELOVL1	hELOVL2	hELOVL3	hELOVL5	hELOVL6	mELOVL3	mELOVL6
activity (IC_{50})	$7.0 \pm 1.7\ \mu M$	$> 10\ \mu M$	130 ± 11 nM	$> 10\ \mu M$	2.6 ± 0.15 nM	19 ± 8.8 nM	14 ± 1.2 nM

[a] Inhibitory activity of (*S*)-**1y** on ELOVLs for their respective substrates. The values represent the mean ± SE for $n \geq 3$.

Table 7. Pharmacokinetic Parameters of (*S*)-**1y** in Sprague−Dawley Rats[a]

	iv (1 mg/kg)				po (3 mg/kg)
CL_p (mL/min/kg)	V_{dss} (L/kg)	$t_{1/2}$ (h)	C_{max} (μM)	$AUC_{0-\infty}$ (μM·h)	F (%)[b]
11	0.7	1.9	2.4	4.69	30

[a] The values represent the mean, $n = 3$ animals. [b] Based on $AUC_{0-\infty}$ values after iv and po administration.

Table 8. Plasma Exposure of (*S*)-**1y** in Mice[a]

time	2 h	4 h	8 h	24 h
plasma level (μM)	11.7	3.7	0.7	ND[b]

[a] The plasma levels were determined after 30 mg/kg oral administration. The values represent the mean for $n = 3$ animals. [b] Not detected.

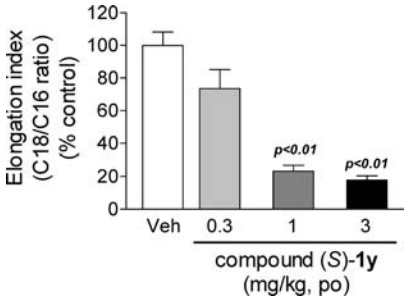

Figure 2. The effect of (*S*)-**1y** on the elongation index of the liver lipids in C57BL/6J mice. The elongation index was determined by the radio-HPLC using [^{14}C]palmitic acid as a radiolabeled substrate and defined as % of control of the ratio of peak area [total amount of C18 fatty acids]/total amount of C16 fatty acids]. Four mice were used for each treatment. See Experimental Section for details.

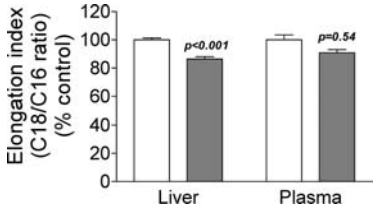

Figure 3. Effects of (*S*)-**1y** on the elongation index of total fatty acids in the liver and plasma of C57BL/6J mice after twice-daily administration for 3 days with vehicle (open column) and 30 mg/kg (*S*)-**1y** (gray column). The elongation index was determined by UV-HPLC after converting fatty acids to corresponding 2-nitrophenylhydrazides and defined as % of control of the ratio of peak area [total amount of C18 fatty acids]/total amount of C16 fatty acids]. Six mice per group were used for each treatment. See Experimental Section for details.

administration. Considering the plasma exposure at 2, 4, 8, and 24 h post 30 mg/kg acute oral dosing of (*S*)-**1y** in mice (Table 8), we administered 30 mg/kg of (*S*)-**1y** twice daily for 3 days to sustain desired plasma levels (i.e., $> 0.54\ \mu M$) throughout the dosing period. Consistent with the inhibitory effect on the [^{14}C]palmitic acid tracer elongation, (*S*)-**1y** significantly decreased the elongation index of total fatty acids in the liver (Figure 3). Similarly, the elongation index of plasma fatty acids tended to decrease but did not reach a statistically significant decrease. Although further studies need to be conducted, considering the fact that both ELOVL3 and ELOVL6 are responsible for the elongation of palmitoyl-CoA, we speculate that (*S*)-**1y** might more potently block the elongation of palmitoyl-CoA than a selective ELOVL6 inhibitor in mice.

Conclusion

In summary, a series of novel and highly potent benzoxazinone derivatives was identified as ELOVL6 inhibitors. Representative compound (*S*)-**1y** showed potent and selective inhibitory activity toward human ELOVL6 while showing dual inhibitory activities toward mouse ELOVL3 and ELOVL6. In the preliminary pharmacodynamic studies, (*S*)-**1y** significantly reduced the elongation index of the liver lipids even at 1 mg/kg p.o. in mice. Furthermore subchronic exposure of (*S*)-**1y** also resulted in a significant decrease of the elongation index of liver fatty acids, demonstrating the utility of (*S*)-**1y** as a pharmacological tool for in vivo studies. At this time, the lack of a selective ELOVL3 inhibitor has limited understanding of physiological roles of ELOVL3 vs ELOVL6. However, further studies using potent mouse ELOVL3/6 dual inhibitor (*S*)-**1y** and available selective ELOVL6 inhibitors[14] would help in understanding the therapeutic applications of ELOVL3 and 6 inhibition, which might lead to the development of novel therapeutics for metabolic disorders.

Experimental Section

Chemistry. General Procedures. Unless otherwise noted, all solvents, chemicals, and reagents were obtained commercially and used without purification. The ^{1}H NMR spectra were obtained at 400 MHz on a MERCURY-400 (Varian) or JMN-AL400 (JEOL) spectrometer, with chemical shifts (δ, ppm) reported relative to TMS as an internal standard. Mass spectra were recorded with electron-spray ionization (ESI) or atmospheric pressure chemical ionization (APCI) on a Waters micromass ZQ, micromass Quattro II, or micromass Q-Tof-2 instrument. Flash chromatography was carried out with prepacked silica gel columns (KP-Sil silica) from Biotage. Preparative thin-layer chromatography was performed on a TLC Silica gel 60 F (Merck KGaA). Preparative HPLC purification was carried out on a YMC-Pack *Pro* C18 (YMC, 30 mm i.d. S-5 μm), eluting with a gradient of CH_3CN/0.1% aqueous CF_3CO_2H at a flow rate of 40 mL/min. Purity of the target compounds was determined by HPLC with the two different eluting methods as follows. Analytical HPLC was performed on a SPELCO Ascentis Express (4.6 mm × 150 mm, s-2.7 μm), eluting with a gradient of (Method A) 0.1% H_3PO_4/CH_3CN = 95/5 to 10/90 over 7 min followed by 10/90 isocratic over 1 min and (Method B) 10 mM potassium phosphate buffer (pH 6.6)/CH_3CN = 95/5 to 20/80 over 7 min followed by 20/80 isocratic over 1 min (detection at 210 nm). Tested compounds had a purity of > 95%, with the exception of **1aa** (94.7%). High-resolution mass spectra were recorded with electron-spray ionization on a micromass Q-Tof-2 instrument. Optical rotation was measured using a 1 mL cell with a 50 mm path length on a JASCO polarimeter P-1020.

1-(5-Bromo-2-fluorophenyl)-2,2,2-trifluoroethanone (3). To a stirred solution of diisopropylamine (56.4 g, 0.55 mol) in THF

(500 mL) was added *n*-BuLi (2.66 M, 200 mL) dropwise at −40 °C, and the resulting mixture was stirred at −40 °C for 1 h and cooled to −78 °C. To the mixture was added 1-bromo-4-fluorobenzene (87.5 g, 0.50 mol) in THF (100 mL) dropwise while keeping the internal temperature below −70 °C, and the mixture was stirred at −78 °C for 1 h. After addition of ethyl trifluoroacetate (65.4 mL, 0.55 mol) in THF (100 mL) at −78 °C, the resultant mixture was allowed to warm to 0 °C, quenched by addition of saturated aqueous NH_4Cl, and partitioned between EtOAc and water. The layers were separated, and the organic layer was washed with brine, dried over $MgSO_4$, and concentrated. The residue was purified by flash silica gel column chromatography (EtOAc/Hexanes = 1/4) to give **3** as a dark yellow oil, which was further purified by distillation under reduced pressure (1 mmHg, 53 °C) to give **3** (83.8 g, 62%) as a yellow oil. ^{1}H NMR (400 MHz, $CDCl_3$): δ 7.15 (1H, dd, J = 10.2, 8.8 Hz), 7.78 (1H, ddd, J = 8.8, 4.4, 2.4 Hz), 7.99 (1H, dd, J = 6.3, 2.4 Hz). MS (ESI) m/z 270 $(M + H)^+$.

1-{5-Bromo-2-[(4-methoxybenzyl)amino]phenyl}-2,2,2-trifluoroethanone (4). A stirred mixture of **3** (76.2 g, 0.281 mol), K_2CO_3 (46.6 g, 0.337 mol), and 4-methoxy benzylamine (73.4 mL, 0.56 mol) in toluene (300 mL) was heated to reflux overnight and cooled to 0 °C. After successive addition of water (300 mL) and citric acid monohydrate (118 g, 0.56 mol), the mixture was stirred at 0 °C for 30 min. The resulting precipitate was collected, dried in vacuo, and suspended in a mixture of 500 mL of hexanes and 10 mL of EtOAc. The suspension was stirred at room temperature for 2 h. The precipitate was collected by filtration and vacuum-dried to give **4** as an orange solid (75.6 g, 69%). The mother liquor was concentrated, and the residue was triturated with a mixture of hexanes and EtOAc to give a second crop (15.9 g, 16%) as a dark brown solid. ^{1}H NMR (400 MHz, $CDCl_3$): δ 3.81 (3H, s), 4.43 (2H, d, J = 5.4 Hz), 6.69 (1H, d, J = 9.3 Hz), 6.89 (2H, d, J = 8.8 Hz), 7.24 (2H, d, J = 8.8 Hz), 7.46 (1H, dd, J = 9.3, 2.0 Hz), 7.87 (1H, dd, J = 4.4, 2.0 Hz), 9.06 (1H, s). MS (ESI) m/z 387 $(M + H)^+$.

6-Bromo-4-ethenyl-1-(4-methoxybenzyl)-4-(trifluoromethyl)-1,4-dihydro-2*H*-3,1-benzoxazin-2-one (5). To a stirred solution of **4** (75.5 g, 0.195 mol) in THF (500 mL) was added vinyl magnesium bromide (1.0 M in THF, 389 mL) at 0 °C dropwise over 1 h, and the mixture was stirred at 0 °C for 3 h. After addition of saturated aqueous NH_4Cl (100 mL), the resultant mixture was stirred at room temperature for 10 min and partitioned between EtOAc and water. The layers were separated, and the organic layer was washed with brine, dried over $MgSO_4$, and concentrated. The residue and triethylamine (81.2 mL, 0.59 mol) were combined in toluene (500 mL) and cooled to 0 °C. To the mixture was added triphosgene (57.9 g, 0.195 mol) portionwise, and the resulting mixture was stirred at 0 °C for 30 min and quenched by addition of saturated aqueous $NaHCO_3$. The mixture was partitioned between EtOAc and water. The layers were separated, and the organic layer was washed with brine, dried over $MgSO_4$, and concentrated. The residual solid was suspended in hexanes (50 mL) and stirred at room temperature overnight. The precipitate was collected by filtration, washed with hexanes, and dried under reduced pressure to give **5** (71.6 g, 83%) as a pale yellow solid. ^{1}H NMR (400 MHz, $CDCl_3$): δ 3.78 (3H, s), 5.10 (2H, s), 5.69 (1H, d, J = 11.2 Hz), 5.72 (1H, d, J = 17.1 Hz), 6.21 (1H, dd, J = 17.1, 11.2 Hz), 6.80 (1H, d, J = 8.8 Hz), 6.86 (2H, d, J = 8.8 Hz), 7.17 (2H, d, J = 8.8 Hz), 7.40 (1H, dd, J = 8.8, 2.0 Hz), 7.45 (1H, s). MS (ESI) m/z 441 $(M + H)^+$.

6-Bromo-4-(hydroxymethyl)-1-(4-methoxybenzyl)-4-(trifluoromethyl)-1,4-dihydro-2*H*-3,1-benzoxazin-2-one (6). Ozone was bubbled through a stirred solution of **5** (71.5 g, 0.161 mol) in CH_2Cl_2 (200 mL) and MeOH (200 mL) at 0 °C for 2 h. After being purged with nitrogen, the mixture was treated with $NaBH_4$ (12.2 g, 0.323 mol) at 0 °C and stirred for 10 min. Volatiles were evaporated under reduced pressure, and the residue was partitioned between EtOAc and 1 N hydrochloric acid (the pH of water layer was adjusted to pH = 6). The layers were separated and the organic layer was washed with brine, dried over $MgSO_4$, and concentrated. The residue was crystallized from EtOH and water to give **6** (62.4 g, 87%) as a colorless solid. ^{1}H NMR (400 MHz, DMSO-d_6): δ 3.71 (3H, s), 3.95 (1H, d, J = 12.2 Hz), 4.33 (1H, d, J = 12.2 Hz), 5.07 (1H, d, J = 16.6 Hz), 5.14 (1H, d, J = 16.6 Hz), 5.81 (1H, brs), 6.90 (2H, d, J = 8.8 Hz), 7.06 (1H, d, J = 8.8 Hz), 7.20 (2H, d, J = 8.8 Hz), 7.60 (1H, dd, J = 8.8, 2.0 Hz), 7.74 (1H, d, J = 2.0 Hz). MS (ESI) m/z 445 $(M + H)^+$.

4-(Azidomethyl)-6-bromo-1-(4-methoxybenzyl)-4-(trifluoromethyl)-1,4-dihydro-2*H*-3,1-benzoxazin-2-one (7). To a stirred solution of **6** (61.3 g, 0.137 mol) and 2,6-dimethylpyridine (48.0 mL, 0.275 mol) in $CHCl_3$ (400 mL) was added trifluoromethanesulfonic anhydride (46.4 mL, 0.275 mol) at 0 °C, and the mixture was stirred 0 °C for 1 h. The reaction was quenched by addition of saturated aqueous $NaHCO_3$. The resulting mixture was partitioned between EtOAc and water. The layers were separated, and the organic layer was successively washed with saturated aqueous NH_4Cl and brine, dried over $MgSO_4$, and concentrated. The residue was combined with NaN_3 (26.7 g, 0.411 mol) in DMF (270 mL) and heated to 80 °C for 3 h. After being cooled to room temperature, the reaction was quenched by addition of water. The resultant mixture was partitioned between EtOAc and water. The layers were separated, and the organic layer was successively washed with 10% aqueous citric acid, water, and brine, then dried over $MgSO_4$, and concentrated. The residue was purified by flash silica gel column chromatography (EtOAc/hexanes = 2/3) to give **7** (46.0 g, 71%) as a colorless solid. ^{1}H NMR (400 MHz, $CDCl_3$): δ 3.77 (3H, s), 3.90 (1H, d, J = 13.7 Hz), 4.09 (1H, d, J = 13.7 Hz), 5.07 (1H, d, J = 16.1 Hz), 5.17 (1H, d, J = 16.1 Hz), 6.84 (1H, d, J = 8.8 Hz), 6.86 (2H, d, J = 8.8 Hz), 7.19 (2H, d, J = 8.8 Hz), 7.33 (1H, s), 7.44 (1H, dd, J = 8.8, 2.4 Hz). MS (ESI) m/z 470 $(M + H)^+$.

4-(Aminomethyl)-6-bromo-1-(4-methoxybenzyl)-4-(trifluoromethyl)-1,4-dihydro-2*H*-3,1-benzoxazin-2-one (8). To a stirred solution of **7** (46.0 g, 98 mmol) in THF (130 mL) and H_2O (65 mL) was added trimethylphosphite (23.1 mL, 195 mmol) at 60 °C, and the mixture was stirred at 60 °C overnight. The resulting mixture was partitioned between EtOAc and water, and the layers were separated. The organic layer was washed with water and brine, dried over $MgSO_4$, and concentrated. The residue was dissolved in 200 mL of a 4 N solution of hydrochloric acid in dioxane and stirred at room temperature for 24 h. Volatiles were removed under reduced pressure, and the residue was partitioned between EtOAc and 2 N aqueous NaOH. The layers were separated, and the organic layer was washed with water and brine, dried over $MgSO_4$, and concentrated to give **8** (30.9 g, 71%) as a colorless solid. ^{1}H NMR (400 MHz, DMSO-d_6): δ 3.21 (1H, d, J = 14.1 Hz), 3.61 (1H, d, J = 14.1 Hz), 3.71 (3H, s), 5.05 (1H, d, J = 16.6 Hz), 5.14 (1H, d, J = 16.6 Hz), 6.89 (2H, d, J = 8.8 Hz), 7.04 (1H, d, J = 8.8 Hz), 7.22 (2H, d, J = 8.8 Hz), 7.59 (1H, dd, J = 8.8, 2.4 Hz), 7.69 (1H, d, J = 2.4 Hz). MS (ESI) m/z 444 $(M + H)^+$.

***N*-{[6-Bromo-1-(4-methoxybenzyl)-2-oxo-4-(trifluoromethyl)-1,4-dihydro-2*H*-3,1-benzoxazin-4-yl]methyl}-4-fluorobenzamide (9).** To a stirred solution of **8** (13.7 g, 30.7 mmol), 4-fluorobenzoic acid (4.73 g, 33.8 mmol), $HOBt \cdot H_2O$ (4.7 g, 30.7 mmol), and triethylamine (4.69 mL, 33.8 mmol) in DMF (50 mL) was added EDCI·HCl (6.47 g, 33.8 mmol) portionwise at 0 °C, and the mixture was allowed to warm up to ambient temperature and stirred overnight. The resultant mixture was diluted with H_2O and stirred for 2 h. The resulting precipitate was collected by filtration, washed with water, and dried under reduced pressure to give **9** (15.6 g, 90%) as a colorless solid. ^{1}H NMR (400 MHz, DMSO-d_6): δ 3.69 (3H, s), 3.91 (1H, dd, J = 14.6, 4.4 Hz), 4.63 (1H, dd, J = 14.6, 7.8 Hz), 5.05 (1H, d, J = 16.6 Hz), 5.13 (1H, d, J = 16.6 Hz), 6.83 (2H, d, J = 8.8 Hz), 7.02 (1H, d, J = 8.8 Hz), 7.17 (2H, d, J = 8.8 Hz), 7.26 (2H, t, J = 8.8 Hz), 7.56 (1H, dd, J = 8.8, 2.4 Hz), 7.63 (1H, s), 7.75 (2H, dd, J = 8.8,

5.4 Hz), 8.87 (1H, dd, J = 7.8, 4.4 Hz). MS (ESI) m/z 566 $(M + H)^+$.

***N*-{[6-Bromo-2-oxo-4-(trifluoromethyl)-1,4-dihydro-2*H*-3,1-benzoxazin-4-yl]methyl}-4-fluorobenzamide (10).** To a stirred solution of **9** (13.0 g, 22.9 mmol) in CH_3CN (50 mL) was added cerium(IV) ammonium nitrate (37.7 g, 68.7 mmol) in water (25 mL) dropwise at room temperature, and the mixture was stirred at room temperature for 4 h. The reaction was quenched by addition of an excess amount of sodium pyrosulfite. After being stirred at room temperature for 30 min, the mixture was partitioned between EtOAc and water, and the layers were separated. The organic layer was washed with water and brine, dried over $MgSO_4$, and concentrated. The residue was crystallized from EtOAc and heptanes to give **10** (9.2 g, 90%) as a colorless solid. ^{1}H NMR (400 MHz, DMSO-d_6): δ 3.85 (1H, d, J = 14.6 Hz), 4.58 (1H, d, J = 14.6 Hz), 6.86 (1H, d, J = 8.8 Hz), 7.26 (2H, t, J = 8.8 Hz), 7.54−7.58 (2H, m), 7.75 (2H, dd, J = 8.8, 5.4 Hz). MS (ESI) m/z 446 $(M + H)^+$.

***N*-{[(4*S*)-6-Bromo-2-oxo-4-(trifluoromethyl)-1,4-dihydro-2*H*-3,1-benzoxazin-4-yl]methyl}-4-fluorobenzamide ((*S*)-10).** **10** was resolved by preparative chiral HPLC (column, AD-H column; eluant, 20% *i*-PrOH in hexanes; flow rate, 1 mL/min) to obtain (*S*)-**10** as the second eluting enantiomer.

4-fluoro-*N*-{[6-iodo-1-(4-methoxybenzyl)-2-oxo-4-(trifluoromethyl)-1,4-dihydro-2*H*-3,1-benzoxazin-4-yl]methyl}benzamide (11). **9** (1.18 g, 2.08 mmol), copper(I) iodide (79 mg, 0.42 mmol), sodium iodide (0.624 g, 4.16 mmol), and *N,N′*-dimethylethylenediamine (89 μL, 0.83 mmol) were combined in 1,4-dioxane (4.2 mL). The mixture was stirred at 110 °C for 4.5 h under a nitrogen atmosphere before being cooled to room temperature. The reaction was quenched by addition of saturated aqueous NH_4Cl. The resultant mixture was partitioned between EtOAc and water. The layers were separated, and the organic layer was washed with brine, dried over $MgSO_4$, and concentrated under reduced pressure. The residue was triturated with EtOAc and hexanes to give **11** (995 mg, 78%) as a colorless solid. ^{1}H NMR (400 MHz, DMSO-d_6): δ 3.68 (3H, s), 3.87 (1H, dd, J = 14.6, 3.9 Hz), 4.61 (1H, dd, J = 14.6, 7.8 Hz), 5.02 (1H, d, J = 16.6 Hz), 5.10 (1H, d, J = 16.6 Hz), 6.83 (2H, d, J = 8.8 Hz), 6.87 (1H, d, J = 8.8 Hz), 7.17 (2H, d, J = 8.8 Hz), 7.25 (2H, t, J = 8.8 Hz), 7.68 (1H, dd, J = 8.8, 2.0 Hz), 7.72−7.77 (3H, m), 8.85 (1H, dd, J = 7.8, 3.9 Hz). MS (ESI) m/z 614 $(M + H)^+$.

[6-Chloro-2-oxo-4-(trifluoromethyl)-1,4-dihydro-2*H*-3,1-benzoxazin-4-yl]methyl-(4-fluorophenyl)carbamate (1a). To a stirred solution of **B** (30 mg, 0.11 mmol) in CH_2Cl_2 (1 mL) was added 1-fluoro-4-isocyanatobenzene (15 mg, 0.11 mmol) and TEA (15 μL, 0.11 mmol) at room temperature, and the mixture was stirred at room temperature for 17 h. Volatiles were removed under reduced pressure, and the residue was purified by preparative HPLC to give **1a** (23 mg, 51%) as a colorless solid. ^{1}H NMR (400 MHz, DMSO-d_6): δ 7.75−7.73 (1H, brm), 7.52 (1H, dd, J = 8.8, 2.2 Hz), 7.44−7.30 (7H, m), 7.00 (1H, d, J = 8.8 Hz), 6.95−6.92 (2H, br m), 5.04 (1H, d, J = 12.2 Hz), 5.04 (2H, s), 4.79 (1H, d, J = 12.2 Hz). MS (ESI) m/z 419 $(M + H)^+$. HRMS $(M + H)^+$ calcd for $C_{17}H_{12}N_2O_4F_4Cl$, 419.0422; found, 419.0426.

1-{[6-Chloro-2-oxo-4-(trifluoromethyl)-1,4-dihydro-2*H*-3,1-benzoxazin-4-yl]methyl}-3-(4-fluorophenyl)urea (1g). Following the procedure described for **1a**, **1g** was prepared from **C** and 1-fluoro-4-isocyanatobenzene. ^{1}H NMR (400 MHz, DMSO-d_6): δ 3.88 (1H, dd, J = 14.6, 5.9 Hz), 4.26 (1H, dd, J = 14.6, 6.8 Hz), 6.44 (1H, t, J = 6.3 Hz), 6.96 (1H, d, J = 8.8 Hz), 7.04 (2H, t, J = 8.8 Hz), 7.27−7.35 (2H, m), 7.49 (1H, dd, J = 8.3, 2.4 Hz), 7.59 (1H, d, J = 2.0 Hz), 8.47 (1H, s), 10.92 (1H, s). MS (ESI) m/z 418 $(M + H)^+$. HRMS $(M + H)^+$ calcd for $C_{17}H_{13}N_3O_3F_4Cl$, 418.0582; found, 418.0594.

1-{[(−)-6-Chloro-2-oxo-4-(trifluoromethyl)-1,4-dihydro-2*H*-3,1-benzoxazin-4-yl]methyl}-3-(4-fluorophenyl)urea ((−)-1g). **1g** was resolved by preparative chiral HPLC (column, AD-H column; eluant, 20% *i*-PrOH in hexanes; flow rate, 1 mL/min) to give (−)-**1g** $([\alpha]_D^{25}$ −51.2 (c 0.13, MeOH)) as the second eluting enantiomer.

***N*-{[6-Chloro-2-oxo-4-(trifluoromethyl)-1,4-dihydro-2*H*-3,1-benzoxazin-4-yl]methyl}-2-(4-fluorophenyl)acetamide (1h).** Following the procedure described for **9**, **1h** was prepared from **C** and (4-fluorophenyl)acetic acid. ^{1}H NMR (400 MHz, CD_3OD): δ 3.22−3.42 (2H, m), 3.63 (1H, d, J = 14.6 Hz), 4.57 (1H, d, J = 14.6 Hz), 6.78−6.91 (3H, m), 6.98 (2H, dd, J = 8.8, 5.4 Hz), 7.27−7.35 (2H, m). MS (ESI) m/z 417 $(M + H)^+$. HRMS $(M + H)^+$ calcd for $C_{18}H_{14}N_2O_3F_4Cl$, 417.0629; found, 417.0632.

***N*-{[6-Chloro-2-oxo-4-(trifluoromethyl)-1,4-dihydro-2*H*-3,1-benzoxazin-4-yl]methyl}-4-fluorobenzamide (1i).** Following the procedure described for **9**, **1i** was prepared from **C** and 4-fluorobenzoic acid. ^{1}H NMR (400 MHz, DMSO-d_6): δ 3.87 (1H, dd, J = 14.4, 4.4 Hz), 4.58 (1H, dd, J = 14.4, 7.6 Hz), 6.92 (1H, d, J = 8.3 Hz), 7.25 (2H, t, J = 9.3 Hz), 7.43−7.50 (2H, m), 7.71−7.78 (2H, m), 8.81 (1H, dd, J = 7.6, 4.4 Hz), 10.19 (1H, s). MS (ESI) m/z 403 $(M + H)^+$. HRMS $(M + H)^+$ calcd for $C_{17}H_{12}N_2O_3F_4Cl$, 403.0473; found, 403.0479.

***N*-{[(+)-6-Chloro-2-oxo-4-(trifluoromethyl)-1,4-dihydro-2*H*-3,1-benzoxazin-4-yl]methyl}-4-fluorobenzamide ((+)-1i) and *N*-{[(−)-6-Chloro-2-oxo-4-(trifluoromethyl)-1,4-dihydro-2*H*-3,1-benzoxazin-4-yl]methyl}-4-fluorobenzamide ((−)-1i).** **1i** was resolved by preparative chiral HPLC (column, AD-H column; eluant, 20% *i*-PrOH in hexanes; flow rate, 1 mL/min) to obtain (+)-**1i** $([\alpha]_D^{25}$ +4.9 (c 0.79, MeOH)) as the first eluting enantiomer and (−)-**1i** $([\alpha]_D^{25}$ −5.7 (c 0.97, MeOH)) as the second eluting enantiomer.

***N*-{[6-Chloro-2-oxo-4-(trifluoromethyl)-1,4-dihydro-2*H*-3,1-benzoxazin-4-yl]methyl}-3-fluorobenzamide (1j).** Following the procedure described for **9**, **1j** was prepared from **C** and 3-fluorobenzoic acid. ^{1}H NMR (400 MHz, DMSO-d_6): δ 3.87 (1H, dd, J = 14.6, 4.4 Hz), 4.57 (1H, dd, J = 14.6, 7.8 Hz), 6.91 (1H, d, J = 8.8 Hz), 7.32−7.39 (1H, m), 7.42−7.53 (6H, m), 8.88 (1H, dd, J = 7.8, 4.4 Hz), 10.87 (1H, s). MS (ESI) m/z 403 $(M + H)^+$. HRMS $(M + H)^+$ calcd for $C_{17}H_{12}N_2O_3F_4Cl$, 403.0473; found, 403.0468.

***N*-{[6-Chloro-2-oxo-4-(trifluoromethyl)-1,4-dihydro-2*H*-3,1-benzoxazin-4-yl]methyl}-2-fluorobenzamide (1k).** Following the procedure described for **9**, **1k** was prepared from **C** and 2-fluorobenzoic acid. ^{1}H NMR (400 MHz, DMSO-d_6): δ 3.86 (1H, dd, J = 14.4, 4.4 Hz), 4.55 (1H, dd, J = 14.4, 7.6 Hz), 6.93 (1H, d, J = 8.8 Hz), 7.16−7.23 (2H, m), 7.29 (1H, td, J = 7.4, 1.8 Hz), 7.42−7.50 (3H, m), 8.78 (1H, dd, J = 7.6, 4.4 Hz), 10.85 (1H, s). MS (ESI) m/z 403 $(M + H)^+$. HRMS $(M + H)^+$ calcd for $C_{17}H_{12}N_2O_3F_4Cl$, 403.0473; found, 403.0467.

***N*-{[6-Chloro-2-oxo-4-(trifluoromethyl)-1,4-dihydro-2*H*-3,1-benzoxazin-4-yl]methyl}-4-methylbenzamide (1l).** Following the procedure described for **9**, **1l** was prepared from **C** and 4-methylbenzoic acid. ^{1}H NMR (400 MHz, DMSO-d_6): δ 2.30 (3H, s), 3.82 (1H, dd, J = 14.6, 4.4 Hz), 4.58 (1H, dd, J = 14.6, 7.8 Hz), 6.90 (1H, d, J = 8.3 Hz), 7.20 (2H, d, J = 8.3 Hz), 7.40−7.48 (2H, m), 7.57 (2H, d, J = 8.3 Hz), 8.69 (1H, dd, J = 7.8, 4.4 Hz), 10.84 (1H, s). MS (ESI) m/z 399 $(M + H)^+$. HRMS $(M + H)^+$ calcd for $C_{18}H_{15}N_2O_3F_3Cl$, 399.0723; found, 399.0726.

***N*-{[6-Chloro-2-oxo-4-(trifluoromethyl)-1,4-dihydro-2*H*-3,1-benzoxazin-4-yl]methyl}-3-methylbenzamide (1m).** Following the procedure described for **9**, **1m** was prepared from **C** and 3-methylbenzoic acid. ^{1}H NMR (400 MHz, DMSO-d_6): δ 2.29 (3H, s), 3.83 (1H, dd, J = 14.6, 4.4 Hz), 4.58 (1H, dd, J = 14.6, 7.8 Hz), 6.91 (1H, d, J = 8.3 Hz), 7.25−7.31 (2H, m), 7.41−7.49 (5H, m), 8.73 (1H, dd, J = 7.8, 4.4 Hz), 10.86 (1H, s). MS (ESI) m/z 399 $(M + H)^+$. HRMS $(M + H)^+$ calcd for $C_{18}H_{15}N_2O_3F_3Cl$, 399.0723; found, 399.0723.

***N*-{[6-Chloro-2-oxo-4-(trifluoromethyl)-1,4-dihydro-2*H*-3,1-benzoxazin-4-yl]methyl}-2-methylbenzamide (1n).** Following the procedure described for **9**, **1n** was prepared from **C** and 2-methylbenzoic acid. ^{1}H NMR (400 MHz, DMSO-d_6): δ 2.01 (3H, s), 3.76 (1H, dd, J = 14.6, 4.4 Hz), 4.62 (1H, dd, J = 14.6, 7.8 Hz), 6.93 (1H, d, J = 8.8 Hz), 7.04−7.06 (1H, m), 7.13−7.16 (2H,

m), 7.23−7.29 (1H, m), 7.47−7.50 (2H, m), 8.75 (1H, dd, J = 7.8, 4.4 Hz), 10.85 (1H, s). MS (ESI) m/z 399 $(M + H)^+$. HRMS $(M + H)^+$ calcd for $C_{18}H_{15}N_2O_3F_3Cl$, 399.0723; found, 399.0726.

***N*-{[6-Chloro-2-oxo-4-(trifluoromethyl)-1,4-dihydro-2*H*-3,1-benzoxazin-4-yl]methyl}-4-methoxybenzamide (1o).** Following the procedure described for **9**, **1o** was prepared from **C** and 4-methoxybenzoic acid. ^{1}H NMR (400 MHz, DMSO-d_6): δ 3.76 (3H, s), 3.81 (1H, dd, J = 14.4, 4.4 Hz), 4.57 (1H, dd, J = 14.4, 7.8 Hz), 6.88−6.95 (3H, m), 7.41−7.45 (2H, m), 7.64−7.68 (2H, m), 8.61 (1H, dd, J = 7.8, 4.4 Hz), 10.84 (1H, s). MS (ESI) m/z 415 $(M + H)^+$. HRMS $(M + H)^+$ calcd for $C_{18}H_{15}N_2O_4F_3Cl$, 415.0672; found, 415.0672.

***N*-{[6-Chloro-2-oxo-4-(trifluoromethyl)-1,4-dihydro-2*H*-3,1-benzoxazin-4-yl]methyl}-4-(trifluoromethyl)benzamide (1p).** Following the procedure described for **9**, **1p** was prepared from **C** and 4-trifluoromethylbenzoic acid. ^{1}H NMR (400 MHz, DMSO-d_6): δ 3.89 (1H, dd, J = 14.6, 4.4 Hz), 4.59 (1H, dd, J = 14.6, 7.8 Hz), 6.91 (1H, d, J = 8.5 Hz), 7.45 (1H, dd, J = 8.5, 2.2 Hz), 7.48 (1H, s), 7.78−7.84 (4H, m), 9.03 (1H, dd, J = 7.8, 4.4 Hz), 10.86 (1H, s). MS (ESI) m/z 453 $(M + H)^+$. HRMS $(M + H)^+$ calcd for $C_{18}H_{12}N_2O_3F_6Cl$, 453.0441; found, 453.0448.

***N*-{[6-Chloro-2-oxo-4-(trifluoromethyl)-1,4-dihydro-2*H*-3,1-benzoxazin-4-yl]methyl}-4-(propan-2-yl)benzamide (1q).** Following the procedure described for **9**, **1q** was prepared from **C** and 4-isopropylbenzoic acid. ^{1}H NMR (400 MHz, DMSO-d_6): δ 1.16 (6H, d, J = 6.8 Hz), 2.84−2.93 (1H, m), 3.82 (1H, dd, J = 14.6, 4.4 Hz), 4.58 (1H, dd, J = 14.6, 7.8 Hz), 6.90 (1H, d, J = 8.3 Hz), 7.26 (2H, d, J = 8.3 Hz), 7.41−7.48 (2H, m), 7.58 (2H, d, J = 8.3 Hz), 8.69 (1H, dd, J = 7.8, 4.4 Hz), 10.84 (1H, s). MS (ESI) m/z 427 $(M + H)^+$. HRMS $(M + H)^+$ calcd for $C_{20}H_{19}N_2O_3F_3Cl$, 427.1036; found, 427.1037.

***N*-{[6-Chloro-2-oxo-4-(trifluoromethyl)-1,4-dihydro-2*H*-3,1-benzoxazin-4-yl]methyl}biphenyl-4-carboxamide (1r).** Following the procedure described for **9**, **1r** was prepared from **C** and 4-phenylbenzoic acid. ^{1}H NMR (400 MHz, DMSO-d_6): δ 3.87 (1H, dd, J = 14.6, 4.4 Hz), 4.62 (1H, dd, J = 14.6, 7.8 Hz), 6.92 (1H, d, J = 8.3 Hz), 7.37−7.49 (5H, m), 7.64−7.79 (6H, m), 8.84 (1H, dd, J = 7.8, 4.4 Hz), 10.86 (1H, s). MS (ESI) m/z 461 $(M + H)^+$. HRMS $(M + H)^+$ calcd for $C_{23}H_{17}N_2O_3F_3Cl$, 461.0880; found, 461.0875.

***N*-{[6-Chloro-2-oxo-4-(trifluoromethyl)-1,4-dihydro-2*H*-3,1-benzoxazin-4-yl]methyl}-4-(methylsulfonyl)benzamide (1s).** Following the procedure described for **9**, **1s** was prepared from **C** and 4-(methanesulfonyl)-benzoic acid. ^{1}H NMR (400 MHz, DMSO-d_6): δ 3.22 (3H, s), 3.89 (1H, dd, J = 14.6, 4.0 Hz), 4.60 (1H, dd, J = 14.6, 7.8 Hz), 6.91 (1H, d, J = 8.8 Hz), 7.45 (1H, dd, J = 8.8, 2.4 Hz), 7.48 (1H, s), 7.86 (2H, dd, J = 6.8, 2.0 Hz), 7.96 (2H, dd, J = 6.8, 2.0 Hz), 9.06 (1H, dd, J = 7.6, 4.0 Hz), 10.87 (1H, s). MS (ESI) m/z 463 $(M + H)^+$. HRMS $(M + H)^+$ calcd for $C_{18}H_{15}N_2O_5F_3SCl$, 463.0342; found,463.0343.

4-Fluoro-*N*-{[2-oxo-4-(trifluoromethyl)-1,4-dihydro-2*H*-3,1-benzoxazin-4-yl]methyl}benzamide (1t). 10 (21 mg, 0.047 mmol) was hydrogenated over 21 mg of 10% Pd/C in a mixture of TEA (10 μL) and THF (1 mL) under an atmospheric pressure of H_2 for 1 h. The mixture was filtered through a pad of Celite, and the filtrate was concentrated. The residual solid was crystallized from EtOH and water to give **1t** (3.0 mg, 17%) as a colorless solid. ^{1}H NMR (400 MHz, DMSO-d_6): δ 3.78 (1H, d, J = 14.7 Hz), 4.57 (1H, d, J = 14.7 Hz), 6.87 (1H, d, J = 8.2 Hz), 7.01 (1H, t, J = 8.0 Hz), 7.20 (2H, t, J = 9.0 Hz), 7.32 (2H, t, J = 8.2 Hz), 7.67−7.71 (2H, m). MS (ESI) m/z 369 $(M + H)^+$. HRMS $(M + H)^+$ calcd for $C_{17}H_{13}N_2O_3F_4$, 369.0862; found, 369.0864.

4-Fluoro-*N*-{[2-oxo-6-phenyl-4-(trifluoromethyl)-1,4-dihydro-2*H*-3,1-benzoxazin-4-yl]methyl}benzamide (1u). Following the procedure described for **1y**, **1u** was prepared from **10** and phenylboronic acid. ^{1}H NMR (400 MHz, DMSO-d_6): δ 3.81 (1H, d, J = 14.6 Hz), 4.85 (1H, dd, J = 14.6, 6.8 Hz), 6.99 (1H, d, J = 8.8 Hz), 7.22 (2H, t, J = 8.8 Hz), 7.35 (1H, t, J = 7.6 Hz), 7.46 (2H, t, J = 7.6 Hz), 7.64−7.68 (4H, m), 7.75 (2H, dd, J = 8.8, 5.4 Hz), 8.89−8.90 (1H, m). MS (ESI) m/z 445 $(M + H)^+$. HRMS $(M + H)^+$ calcd for $C_{23}H_{17}N_2O_3F_4$, 445.1175; found, 445.1184.

4-Fluoro-*N*-{[2-oxo-6-(2-oxopyridin-1(2*H*)-yl)-4-(trifluoromethyl)-1,4-dihydro-2*H*-3,1-benzoxazin-4-yl]methyl}benzamide (1v). Following the procedure described for **1ab**, **1v** was prepared from **11** and pyridin-2(1*H*)-one. ^{1}H NMR (400 MHz, DMSO-d_6): δ 3.86 (1H, dd, J = 14.6, 4.4 Hz), 4.59 (1H, dd, J = 14.6, 7.8 Hz), 6.34 (1H, td, J = 6.8, 1.5 Hz), 6.47 (1H, dd, J = 9.8, 1.5 Hz), 6.97 (1H, d, J = 9.3 Hz), 7.24 (2H, t, J = 8.8 Hz), 7.45−7.52 (4H, m), 7.74 (2H, dd, J = 8.8, 5.4 Hz), 8.82 (1H, dd, J = 7.8, 4.4 Hz), 10.90 (1H, s). MS (ESI) m/z 462 $(M + H)^+$. HRMS $(M + H)^+$ calcd for $C_{22}H_{16}N_3O_4F_4$, 462.1077; found, 462.1077.

4-Fluoro-*N*-{[6-(isoxazol-4-yl)-2-oxo-4-(trifluoromethyl)-1,4-dihydro-2*H*-3,1-benzoxazin-4-yl]methyl}benzamide (1w). Following the procedure described for **1y**, **1w** was prepared from **10** and 4-(4,4,5,5-tetramethyl-1,3,2-dioxaborolan-2-yl)isoxazole. ^{1}H NMR (400 MHz, DMSO-d_6): δ 3.95 (1H, d, J = 14.5 Hz), 4.59 (1H, d, J = 14.5 Hz), 6.92 (1H, d, J = 8.2 Hz), 7.19 (2H, t, J = 8.9 Hz), 7.64−7.71 (3H, m), 7.74 (1H, brs), 9.04 (1H, brs), 9.32 (1H, brs). MS (ESI) m/z 436 $(M + H)^+$. HRMS $(M + H)^+$ calcd for $C_{20}H_{14}N_3O_4F_4$, 436.0920; found, 436.0915.

4-Fluoro-*N*-{[2-oxo-6-(1*H*-pyrazol-4-yl)-4-(trifluoromethyl)-1,4-dihydro-2*H*-3,1-benzoxazin-4-yl]methyl}benzamide (1x). Following the procedure described for **1y**, **1x** was prepared from **10** and 4-(4,4,5,5-tetramethyl-1,3,2-dioxaborolan-2-yl)-1*H*-pyrazole. ^{1}H NMR (400 MHz, DMSO-d_6): δ 3.87 (1H, dd, J = 14.1, 3.9 Hz), 4.72 (1H, dd, J = 14.1, 8.3 Hz), 6.89 (1H, dd, J = 8.3, 1.5 Hz), 7.22 (2H, t, J = 8.8 Hz), 7.57 (1H, dd, J = 8.3, 1.5 Hz), 7.61 (1H, brs), 7.72 (2H, dd, J = 8.8, 5.4 Hz), 7.96 (2H, brs), 8.83 (1H, dd, J = 8.3, 3.9 Hz), 10.68 (1H, s). MS (ESI) m/z 435 $(M + H)^+$. HRMS $(M + H)^+$ calcd for $C_{20}H_{15}N_4O_3F_4$, 435.1080; found,435.1086.

4-Fluoro-*N*-{[(+)-2-oxo-6-(1*H*-pyrazol-4-yl)-4-(trifluoromethyl)-1,4-dihydro-2*H*-3,1-benzoxazin-4-yl]methyl}benzamide ((+)-1x). **1x** was resolved by preparative chiral HPLC (column, AD-H column; eluant, 20% *i*-PrOH in hexanes; flow rate, 1 mL/min) to obtain (+)-**1x** ($[\alpha]_D^{25}$ +63.0 (c 0.42, MeOH)) as the second eluting enantiomer.

4-Fluoro-*N*-{[2-oxo-6-(1*H*-pyrazol-5-yl)-4-(trifluoromethyl)-1,4-dihydro-2*H*-3,1-benzoxazin-4-yl]methyl}benzamide (1y). 10 (4.0 g, 8.94 mmol), [1-(tetrahydro-2*H*-pyran-2-yl)-1*H*-pyrazol-5-yl]boronic acid (2.63 g, 13.42 mmol), $PdCl_2$(dppf) (654 mg, 0.894 mmol), and potassium phosphate trihydrate (4.76 g, 17.88 mmol) were combined in a mixture of DMF (27 mL) and water (2.7 mL) at room temperature, and the mixture was stirred at 120 °C for 15 min under microwave irradiation. After being cooled to room temperature, the mixture was treated with water (10 mL) and conc hydrochloric acid (5 mL) and stirred at room temperature for 2 h. The resulting mixture was partitioned between EtOAc and water, and the layers were separated. The organic layer was washed with water and brine, dried over $MgSO_4$, and concentrated under reduced pressure. The residue was purified by flash silica gel column chromatography (EtOAc/hexanes = 1/1) to give **1y** (2.7 g, 70%) as a colorless solid. ^{1}H NMR (400 MHz, DMSO-d_6): δ 3.90 (1H, dd, J = 14.6, 3.9 Hz), 4.66 (1H, dd, J = 14.6, 7.3 Hz), 6.65 (1H, d, J = 2.0 Hz), 6.95 (1H, d, J = 8.8 Hz), 7.21 (2H, t, J = 8.8 Hz), 7.70−7.80 (5H, m), 8.82 (1H, dd, J = 7.3, 3.9 Hz), 12.92 (1H, brs). MS (ESI) m/z 435 $(M + H)^+$. HRMS $(M + H)^+$ calcd for $C_{20}H_{15}N_4O_3F_4$, 435.1080; found,435.1087.

4-Fluoro-*N*-{[(+)-(4*S*)-2-oxo-6-(1*H*-pyrazol-5-yl)-4-(trifluoromethyl)-1,4-dihydro-2*H*-3,1-benzoxazin-4-yl]methyl}benzamide ((*S*)-1y). **1y** was resolved by preparative chiral HPLC (column, AD-H column; eluant, 20% *i*-PrOH in hexanes; flow rate, 1 mL/min) to obtain (*S*)-**1y** ($[\alpha]_D^{25}$ +84.2 (c 1.2, MeOH)) as the second eluting enantiomer. And also following the same procedure to prepare **1y**, (*S*)-**1y** was prepared from (*S*)-**10**.

4-Fluoro-*N*-{[2-oxo-6-(1*H*-pyrazol-1-yl)-4-(trifluoromethyl)-1,4-dihydro-2*H*-3,1-benzoxazin-4-yl]methyl}benzamide (1z). Following the procedure described for **1ab**, **1z** was prepared from **11** and pyrazole. ^{1}H NMR (400 MHz, DMSO-d_6): δ 3.94 (1H, dd, J = 14.4, 4.9 Hz), 4.63 (1H, dd, J = 14.4, 7.3 Hz), 6.55 (1H, t, J = 2.4 Hz), 7.00 (1H, d, J = 8.8 Hz), 7.21 (2H, t, J = 8.8 Hz), 7.69−7.73 (3H, m), 7.82−7.86 (2H, m), 8.39 (1H, d, J = 2.4 Hz), 8.83 (1H, dd, J = 7.3, 4.9 Hz), 10.84 (1H, s). MS (ESI) m/z 435 (M + H)$^+$. HRMS (M + H)$^+$ calcd for $C_{20}H_{15}N_4O_3F_4$, 435.1080; found, 435.1089.

4-Fluoro-*N*-{[(+)-2-oxo-6-(1*H*-pyrazol-1-yl)-4-(trifluoromethyl)-1,4-dihydro-2*H*-3,1-benzoxazin-4-yl]methyl}benzamide ((+)-1z). **1z** was separated by preparative chiral HPLC (column, AD-H column; eluant, 20% *i*-PrOH in hexanes; flow rate, 1 mL/min) to give (+)-**1z** ($[\alpha]_D^{25}$ +71.7 (c 0.38, MeOH)) as the second eluting enantiomer.

4-Fluoro-*N*-{[2-oxo-6-(1*H*-1,2,4-triazol-5-yl)-4-(trifluoromethyl)-1,4-dihydro-2*H*-3,1-benzoxazin-4-yl]methyl}benzamide (1aa). Following the procedure described for **1ac**, **1aa** was prepared from **10** and 1-[(benzyloxy)methyl]-1*H*-1,2,4-triazole. HPLC purity (94.7%); ^{1}H NMR (400 MHz, DMSO-d_6): δ 3.95 (1H, dd, J = 14.4, 4.4 Hz), 4.52 (1H, dd, J = 14.4, 7.3 Hz), 7.00 (1H, d, J = 8.3 Hz), 7.20 (2H, t, J = 8.8 Hz), 7.69 (2H, dd, J = 8.8, 5.4 Hz), 7.99 (1H, dd, J = 8.3, 2.0 Hz), 8.05 (1H, brs), 8.42 (1H, brs), 8.79 (1H, dd, J = 7.3, 4.4 Hz). MS (ESI) m/z 436 (M + H)$^+$. HRMS (M + H)$^+$ calcd for $C_{19}H_{14}N_5O_3F_4$, 436.1033; found, 436.1034.

4-Fluoro-*N*-{[2-oxo-6-(1*H*-1,2,4-triazol-1-yl)-4-(trifluoromethyl)-1,4-dihydro-2*H*-3,1-benzoxazin-4-yl]methyl}benzamide (1ab). **11** (50 mg, 0.081 mmol), 1,2,4-triazole (16.9 mg, 0.244 mmol), potassium phosphate (25.9 mg, 0.122 mmol), copper iodide (3.1 mg, 0.016 mmol) and *N*,*N*′-dimethylethylenediamine (6.9 μL, 0.065 mmol) were combined in DMF (0.4 mL), and the resultant mixture was stirred at 110 °C for 1 h under a nitrogen atmosphere before being cooled to room temperature, The reaction was quenched by addition of saturated aqueous NH_4Cl. The resulting mixture was partitioned between EtOAc and water, and the layers were separated. The organic layer was washed with brine, dried over $MgSO_4$, and concentrated under reduced pressure. The residual oil and aluminum chloride (107 mg, 0.80 mmol) were combined in anisole (0.43 mL) at room temperature, and the mixture was stirred at 100 °C for 2 h. After being cooled to room temperature, the reaction was quenched by addition of saturated aqueous $NaHCO_3$. The mixture was partitioned between EtOAc and water, and the layers were separated. The organic layer was washed with brine, dried over $MgSO_4$, and concentrated under reduced pressure. The residue was purified by preparative TLC (hexanes/EtOAc = 1/1) followed by preparative HPLC to provide **1ab** (5.2 mg, 15% in 2 steps) as a colorless solid. ^{1}H NMR (400 MHz, DMSO-d_6): δ 3.99 (1H, dd, J = 14.6, 4.4 Hz), 4.59 (1H, dd, J = 14.6, 6.8 Hz), 7.05 (1H, d, J = 8.8 Hz), 7.21 (2H, t, J = 8.8 Hz), 7.70 (2H, dd, J = 8.8, 5.4 Hz), 7.85 (1H, dd, J = 8.8, 2.4 Hz), 7.95 (1H, s), 8.23 (1H, s), 8.81 (1H, dd, J = 6.8, 4.4 Hz), 9.18 (1H, s), 10.94 (1H, s). MS (ESI) m/z 436 (M + H)$^+$. HRMS (M + H)$^+$ calcd for $C_{19}H_{14}N_5O_3F_4$, 436.1033; found, 436.1030.

4-Fluoro-*N*-{[6-(1*H*-imidazol-2-yl)-2-oxo-4-(trifluoromethyl)-1,4-dihydro-2*H*-3,1-benzoxazin-4-yl]methyl}benzamide (1ac). To a stirred solution of 1-[(benzyloxy)methyl]-1*H*-imidazole (105 mg, 0.56 mmol) in THF (0.3 mL) was added *n*-BuLi (2.4 M in hexanes, 233 μL) at −78 °C. After 30 min, zinc bromide (151 mg, 0.67 mmol) was added, and the mixture was stirred at −78 °C for an additional 30 min and allowed to warm to room temperature. To the mixture was added **10** (100 mg, 0.224 mmol), $Pd(PPh_3)_4$ (25.8 mg, 0.022 mmol), and DMF (0.5 mL) at room temperature, and the mixture was stirred at 80 °C for 2 h before being cooled to room temperature. The reaction was quenched by addition of saturated aqueous $NaHCO_3$. The mixture was partitioned between EtOAc and water. The layers were separated, and the organic layer was washed with brine, dried over $MgSO_4$, and concentrated under reduced pressure. The residue was combined with aluminum chloride (271 mg, 2.0 mmol) in anisole (1.0 mL) at room temperature, and the mixture was stirred at 100 °C for 2 h. The reaction was quenched by addition of saturated aqueous $NaHCO_3$ at room temperature. The resultant mixture was partitioned between EtOAc and water, and the layers were separated. The organic layer was washed with brine, dried over $MgSO_4$, and concentrated under reduced pressure. The residue was purified by preparative HPLC to give **1ac** (13.3 mg, 14% in 2 steps) as a colorless solid. ^{1}H NMR (400 MHz, DMSO-d_6): δ 4.08 (1H, dd, J = 14.1, 4.9 Hz), 4.42 (1H, dd, J = 14.1, 6.3 Hz), 6.96 (2H, d, J = 8.8 Hz), 7.21 (3H, t, J = 8.8 Hz), 7.23 (1H, brs), 7.71 (2H, dd, J = 8.8, 5.4 Hz), 7.92 (1H, dd, J = 8.8, 1.5 Hz), 8.02 (1H, brs), 8.74−8.77 (1H, brm), 10.81 (1H, brs), 12.50 (1H, s). MS (ESI) m/z 435 (M + H)$^+$. HRMS (M + H)$^+$ calcd for $C_{20}H_{15}N_4O_3F_4$, 435.1080; found, 435.1078.

4-Fluoro-*N*-{[2-oxo-6-(2-oxopyrrolidin-1-yl)-4-(trifluoromethyl)-1,4-dihydro-2*H*-3,1-benzoxazin-4-yl]methyl}benzamide (1ad). Following the procedure described for **1ab**, **1ad** was prepared from **11** and pyrrolidin-2-one. ^{1}H NMR (400 MHz, DMSO-d_6): δ 1.99−2.07 (2H, m), 2.43−2.48 (2H, m), 3.69−3.81 (2H, m), 3.85 (1H, dd, J = 14.6, 4.4 Hz), 4.56 (1H, dd, J = 14.6, 7.8 Hz), 6.89 (1H, d, J = 8.8 Hz), 7.23 (2H, t, J = 8.8 Hz), 7.50 (1H, d, J = 2.0 Hz), 7.74 (2H, dd, J = 8.8, 5.9 Hz), 7.79 (1H, dd, J = 8.8, 2.4 Hz), 8.78 (1H, dd, J = 7.8, 4.4 Hz), 10.67 (1H, s). MS (ESI) m/z 452 (M + H)$^+$. HRMS (M + H)$^+$ calcd for $C_{21}H_{18}N_3O_4F_4$, 452.1233; found, 452.1240.

4-Fluoro-*N*-{[2-oxo-6-(2-oxo-1,3-oxazolidin-3-yl)-4-(trifluoromethyl)-1,4-dihydro-2*H*-3,1-benzoxazin-4-yl]methyl}benzamide (1ae). Following the procedure described for **1ab**, **1ae** was prepared from **11** and 1,3-oxazolidin-2-one. ^{1}H NMR (400 MHz, DMSO-d_6): δ 3.85 (1H, dd, J = 14.6, 4.4 Hz), 3.95 (1H, q, J = 8.3 Hz), 4.05 (1H, q, J = 8.3 Hz), 4.42 (2H, t, J = 8.3 Hz), 4.57 (1H, dd, J = 14.6, 7.8 Hz), 6.92 (1H, d, J = 8.8 Hz), 7.22 (2H, t, J = 8.8 Hz), 7.45 (1H, d, J = 2.4 Hz), 7.68 (1H, dd, J = 8.8, 2.4 Hz), 7.74 (2H, dd, J = 8.8, 5.9 Hz), 8.79 (1H, dd, J = 7.8, 4.4 Hz), 10.68 (1H, s). MS (ESI) m/z 454 (M + H)$^+$. HRMS (M + H)$^+$ calcd for $C_{20}H_{16}N_3O_5F_4$, 454.1026; found, 454.1026.

Biology. Reagents. Glucose-6-phosphate, β-nicotinamide-adenine dinucleotide phosphate and glucose-6-phosphate dehydrogenase were purchased from Oriental Yeast Co., Ltd. (Tokyo, Japan). [^{14}C]-Malonyl-CoA was purchased from GE Healthcare Science (Little Chalfont, UK). [^{14}C]-Palmitoyl-CoA was purchased from PerkinElmer Japan (Kanagawa, Japan). [^{14}C]-Stearoyl-CoA was purchased from Muromachi-Yakuhin (Tokyo, Japan). The oligonucleotide primers were purchased from Hokkaido System Science (Hokkaido, Japan). Human and mouse liver microsomes were obtained from BD Biosciences (San Jose, CA) and XENOTECH (Lenexa, KS), respectively. Other reagents were obtained from Sigma (St. Louis, MO). Male C57BL/6J mice (5−7 weeks of age) and male SD rats (5−7 weeks of age) were purchased from CLEA Japan (Tokyo, Japan) and Charles River Japan, respectively (Kanagawa, Japan).

Cloning and Expression of hELOVL6. The hELOVL6 coding sequence (accession number: NP_076995) was amplified by RT-PCR from human liver cDNA library (Clontech) using the following primers: 5′ primer, 5′-GGATCCAACATGT-CAGTGTTGACTT-3′ and 3′ primer, 5′-CTCGAGCTATT-CAGCTTTCGTTGTT-3′. Cloned DNA sequence was ligated with the double-digested pPICZαB vector (Invitrogen). The integrity of all PCR products and ligations was confirmed by DNA sequencing.

Preparation of the Microsome Fraction Expressing hELOVL6. The pPICZα-FLAG-rhELOVL6 expression vector was transformed into the *Pichia pastoris* SMD1168 yeast strain using the Pichia EasyComp Transformation Kit (Invitrogen). The transformants were selected on YPDS plates (1% yeast extract, 2% peptone, 2% dextrose, and 1 M sorbitol) containing 100 μg/mL of Zeocin. The cells were grown in BMGY medium

(1% yeast extract, 2% peptone, 100 mM potassium phosphate pH 6.0, 1.34% yeast nitrogen base, (4×10^{-5})% biotin, and 1% glycerol). Expression of the α-factor signal sequence/FLAG/hELOVL6 fusion protein was induced in BMMY medium (1% glycerol is replaced with 0.5% methanol), and the cells were cultured for 48 h at 30 °C in a rotary shaker (180 rpm). Preparation of the microsome fraction was performed at 4 °C. In brief, the yeast cells were harvested by centrifugation at 3000 *g* for 10 min and washed with cold breaking buffer (50 mM potassium phosphate (pH 7.4), 1 mM EDTA, 5% glycerol, and 1 tablet/50 mL of protease inhibitor cocktail (Roche)). The cells were then vigorously broken with glass beads in cold breaking buffer. The resultant homogenate was centrifuged at 10 000 *g* for 10 min, and the supernatant was further centrifuged at 100 000 *g* for 1 h at 4 °C. The pellet was suspended in resuspension buffer (50 mM Tris-HCl (pH 7.4), 1 mM EDTA, 20% glycerol, and 1 tablet/50 mL of protease inhibitor cocktail), and again centrifuged at 100 000 *g* for 1 h at 4 °C. The pellet was suspended in the resuspension buffer and used as the microsomal fraction (FLAG-rhELOVL6 microsome) for the elongase assay.

Cloning and Expression of ELOVL Family. The human or mouse ELOVL family coding sequence was amplified by RT-PCR from human or mouse liver cDNA library (Clontech) described in previous reports.[14a] Cloned DNA sequence was ligated with the double-digested pPICZαB vector (Invitrogen). The integrity of all PCR products and ligations was confirmed by DNA sequencing.

Preparation of the Microsome Fraction Expressing ELOVL. The pPICZα-FLAG-rELOVL expression vector was transformed into the *Pichia pastoris* SMD1168 yeast strain using the Pichia EasyComp Transformation Kit (Invitrogen). Microsome fraction was prepared from each transformants as the enzyme source for the elongase assay of each ELOVL family.

ELOVL6 in Vitro Enzyme Assay. The long chain fatty acyl-CoA elongation assay was performed as described elsewhere (Kitazawa, Miyamoto et al., submitted for publication). Briefly, 30 μL of the reaction mixture (100 mM potassium phosphate buffer (pH 6.5), 200 μM BSA (fatty acid free), 500 μM NADPH, 1 μM rotenone, 20 μM malonyl-CoA, 833 kBq/mL [^{14}C]-malonyl-CoA, and 40 μM palmitoyl-CoA) was used as the substrate mixture. To start reaction, 20 μL of the ELOVL6 microsomal protein (3 μg) was added to the substrate mixture, and then incubated for 1 h at 37 °C with gentle shaking. This reaction step was performed in a 96-well plate. After 1 h incubation, 100 μL of 5 N HCl was added for the hydrolysis of acyl-CoAs, and then the reaction mixture was filtered through a Unifilter-96, GF/C plate (PerkinElmer, Waltham, MA) using a FilterMate cell harvester (PerkinElmer, Waltham, MA). The 96-well GF/C filter plate was subsequently washed with distilled water to remove excess [^{14}C]-malonyl-CoA and dried, after which 25 μL of MICROSCINT 0 was added to each well and radioactivity was measured using TopCount (PerkinElmer, Waltham, MA). For other ELOVL subtypes, corresponded acyl-CoA as indicated below instead of palmitoyl-CoA was used for respective enzyme assay: ELOVL1, 10 μM stearoyl-CoA; ELOVL2, 10 μM arachidonoyl-CoA; ELOVL3, 10 μM stearoyl-CoA; ELOVL5, 40 μM arachidonoyl-CoA. For an enzyme inhibition assay, indicated concentrations of test compounds or control vehicle (DMSO: final concentration 1.0%) was included in the substrate mixture. Residual enzyme activity was determined as the percentage of the respective control. All data including IC_{50} values were analyzed by nonlinear regression using GraphPad Prism version 4.00 (GraphPad Software, Inc.).

In Vitro Hepatocyte Assay. Mouse hepatoma H2.35 cells were grown on 24-well plates in Dulbecco's modified Eagle's medium (DMEM) (Invitrogen, Carlsbad, CA) supplemented with 200 nM dexamethasone and 4% heat-inactivated fetal bovine serum (FBS) at 33 °C under 5% CO_2 in a humidified incubator. The test compound dissolved in medium was incubated with subconfluent H2.35 cells for 60 min at 33 °C. [1-^{14}C]-palmitic acid (16:0) was added to each well to a final concentration of 0.8 μCi/mL to detect elongase activity. After 4 h incubation at 33 °C, the culture medium was removed, and the labeled cells were washed with chilled PBS (3 × 0.5 mL) and dissolved in 250 μL of 2 N sodium hydroxide. The cell lysate was incubated at 70 °C for 1 h to hydrolyze radio labeled cellular lipids. After acidification with 100 μL of 5 N HCl, fatty acids were extracted with 300 μL of acetonitrile. Radiolabeled palmitic acid (16:0), palmitoleic acid (16:1), stearic acid (18:0), and *cis*-vaccenic acid (18:1,n-7) and oleic acid (18:1,n-9) were quantified by reversed-phase HPLC with a Packard Flow Scintillation Analyzer 500TR (radio-HPLC) (Amersham Biosciences, Piscataway, NJ). The identity of the labeled fatty acids was determined by comparing the retention times with known fatty acid standards. Elongation activity was monitored as the elongation index. The elongation index was defined as follows: Elongation index = total amount of C18 fatty acids/total amount of C16 fatty acids = [stearoyl acid + oleic acid + *cis*-vaccenic acid]/[palmitic acid + palmitoleic acid].

In Vivo [^{14}C]-Palmitoyl-CoA Elongation. Male C57BL/6J mice (CLEA Japan) and SD rats (Charles River Japan) were individually housed in plastic cages with ad libitum access to normal rodent chow (CE2, CLEA Japan) and water. (*S*)-**1y** (dissolved in 0.5% methylcellulose) was orally administered to mice, and 1 h later, [1-^{14}C]-palmitic acid was interperitoneally administered at 10 μCi/body. At 2 h postdosing of (*S*)-**1y**, animals were anesthetized with isoflurane (4%) and killed by blood collection from the vena cava. 50 mg of the liver was harvested and incubated in potassium hydroxide/ethanol (2 mL/1.4 mL) at 70 °C for 1 h. The nonacid-lipid was extracted by 4 mL of petroleum ether and discarded. Fatty acids were extracted by 2 mL of petroleum ether following saponification by 2 mL of 6 N HCl. The ether phase containing fatty acids fraction was evaporated under nitrogen gas and reconstituted in methanol to measure the radioactivity by radio-HPLC. The radioactivity corresponding to each fatty acid was quantified to calculate the elongation index as described above. All animal procedures were conducted according to protocols and guidelines approved by the Banyu Institutional Animal Care and Use Committee.

Fatty Acid Composition in Liver and Plasma. (*S*)-**1y** was administered orally twice daily at 30 mg/kg for 3 days to male C57BL/6J mice, and then the mice were anesthetized and tissues immediately isolated, weighed, frozen in liquid nitrogen and stored at −80 °C until use. The liver samples were incubated in 100-fold volume (w/v) of 5 N NaOH/ethanol (1:1) at 60 °C. After 2 h incubation, 500 μL of 5 N HCl and C17:0 (internal standard) fatty acid was added to all hydrolysates. For plasma samples, 50 μL of the plasma samples were incubated in 200 μL of 5 N NaOH/ethanol (1:1), 10 μL of C17:0 fatty acid, and 100 μL of 5 N HCl. The fatty acid composition was analyzed by a previously described method[24] with slight modifications. Briefly, the fatty acids in the tissue hydrolysate were derivatized with 2-nitrophenylhydrazine, and these derivatives were purified using an Oasis HLB column. An aliquot (10 μL) of the eluate was injected into the HPLC apparatus for analysis. HPLC analysis was performed with a Shimadzu 10Avp system (Shimadzu, Kyoto, Japan), equipped with a UV detector (SPD-10Avp), two pumps (LC-10ADvp), an autosampler (SIL-10ADvp), and a column oven (CTO-10ACvp). The mobile phase consisted of CH_3CN-water (80:20, flow rate, 0.6 mL/min). The separation was performed with a CAPCELL PAK C18 MGII (2.0 mm i.d. × 150 mm, 5 μm) at 35 °C, and the UV absorbance was subsequently measured at 400 nm. The elongation index represented the ratio of total amount of C18 fatty acids to total amount of C16 fatty acids, which was quantified from each fatty acid amount.

Plasma Protein Binding in Mice Plasma. Mouse (C57BL/6N) plasma fraction was prepared by standard procedure and its pH was adjusted to 7.4 just prior to use. Plasma protein binding was

determined by an equilibrium dialysis method using reusable 96-well Micro-Equilibrium Dialysis Device HTD 96b (HT-Dialysis LLC). In brief, each well was separated by a dialysis membrane (HTD 96a/b Dialysis Membrane Strips, MWCO 12 000−14 000, HTDialysis LLC) soaked in PBS (phosphate buffered saline, purchased from Invitrogen Japan, Inc.) to produce two side-by-side chambers, plasma side and buffer side. Plasma (150 μL) containing 1 μM of test compounds and PBS (150 μL) were placed in the plasma side and the buffer side, respectively. All assay wells were sealed and incubated at 37 °C with gentle agitation. After 6 h incubation, aliquots (50 μL) of plasma and dialysate (PBS) sample were transferred to polypropylene tubes and mixed with 150 μL of ethanol containing internal standard. The all samples were centrifuged at 10 000*g* for 10 min at 4 °C, and the resultant supernatants were analyzed by LC-MS/MS. Percentage of plasma protein unbound fraction was calculated as follows: Unbound fraction (%) = Cf/Cp × 100, where Cf and Cp represent the drug concentration on the buffer side and the plasma side post equilibrium, respectively.

Plasma and Liver Exposure in Mice. Pharmacokinetic characterization was conducted in male C57BL/6J mice following single oral administration of (*S*)-**1y**. Single doses of (*S*)-**1y** at 10 or 30 mg/kg body weight were administered orally by gavage in a vehicle of 0.5% methylcellulose aqueous suspension. Blood samples from the abdominal vein and liver samples were obtained 2 h after 10 mg/kg oral administration. Blood samples for the determination of drug plasma concentrations were obtained at multiple time points up to 24 h after 30 mg/kg oral administration. Blood samples were centrifuged to separate the plasma. Liver samples were homogenized with phosphate-buffered saline (pH 7.4). Each sample was deproteinized with ethanol containing an internal standard. (*S*)-**1y** and the internal standard were detected by liquid chromatography mass spectrometry/mass spectrometry (LC-MS/MS) in positive ionization mode using an electrospray ionization probe, and their precursor to production combinations were monitored using the Multiple Reaction Monitoring mode.

Pharmacokinetics in SD Rats. Pharmacokinetics characterization in SD rats was conducted following single oral and single intravenous administration. Single doses of (*S*)-**1y** were administered either intravenously in a vehicle of PEG400/EtOH/H_2O = 50/10/40 or orally by gavage in a vehicle of 0.5% methylcellurose aqueous suspension. Doses of 1 and 3 mg/kg were used for iv and po, respectively. Blood samples for the determination of drug plasma concentrations were obtained at multiple time points up to 24 h after administration. Blood samples were centrifuged to separate the plasma, and the plasma samples were deproteinized with ethanol containing an internal standard. Compound (*S*)-**1y** and the internal standard were detected by LC-MS/MS in a positive ionization mode using the electrospray ionization probe, and their precursor to product ion combinations were monitored in Multiple Reaction Monitoring mode.

Acknowledgment. We thank Naomi Morita and Dr. Tomoyuki Ohe for collecting pharmacokinetic and plasma unbound fraction data, Hiroaki Suwa for HPLC purity analysis and Hirokazu Ohsawa for mass spectra analysis and Dr. Michael McNevin and Dr. Richard G Ball for determination of the absolute configuration of (*S*)-**10**. We also thank Dr. Peter T. Meinke (Merck Research Laboratories, Rahway, NJ) for the editing of this manuscript.

Supporting Information Available: Synthetic procedures for **1b**−**f** and intermediates **A**−**F**, and experimental details of X-ray crystallography analysis of (*S*)-**10**. This material is available free of charge via the Internet at http://pubs.acs.org.

References

(1) Unger, R. H. Mini review: weapons of lean body mass destruction: the role of ectopic lipids in the metabolic syndrome. *Endocrinology* **2003**, *144*, 5159–5165.
(2) Delarue, J; Magnan, C. Free fatty acids and insulin resistance. *Curr. Opin. Clin. Nutr. Metab. Care* **2007**, *10*, 142–148.
(3) Cao, H.; Gerhold, K.; Mayers, J. R.; Wiest, M. M.; Watkins, S. M.; Hotamisligil, G. S. Identification of a lipokine, a lipid hormone linking adipose tissue to systemic metabolism. *Cell* **2008**, *134*, 933–944.
(4) Matsuzaka, T.; Shimano, H.; Yahagi, N.; Kato, T.; Atsumi, A.; Yamamoto, T.; Inoue, N.; Ishikawa, M.; Okada, S.; Ishigaki, N.; Iwasaki, H.; Iwasaki, Y.; Karasawa, T.; Kumadaki, S.; Matsui, T.; Sekiya, M.; Ohashi, K.; Hasty, A. H.; Nakagawa, Y.; Takahashi, A.; Suzuki, H.; Yatoh, S.; Sone, H.; Toyoshima, H.; Osuga, J.; Yamada, N. Crucial role of a long-chain fatty acid elongase, Elovl6, in obesity-induced insulin resistance. *Nat. Med.* **2007**, *13*, 1193–1202.
(5) Barrett, P. B.; Harwood, J. L. Characterization of fatty acid elongase enzymes from germinating pea seeds. *Phytochemistry* **1998**, *48*, 1295–1304.
(6) Nugteren, D. H. The enzymic chain elongation of fatty acids by rat-liver microsomes. *Biochim. Biophys. Acta* **1965**, *106*, 280–290.
(7) Matsuzaka, T.; Shimano, H.; Yahagi, N.; Yoshikawa, T.; Amemiya-Kudo, M.; Hasty, A. H.; Okazaki, H.; Tamura, Y.; Iizuka, Y.; Ohashi, K.; Osuga, J.; Takahashi, A.; Yato, S.; Sone, H.; Ishibashi, S.; Yamada, N. Cloning and characterization of a mammalian fatty acyl-CoA elongase as a lipogenic enzyme regulated by SREBPs. *J. Lipid Res.* **2002**, *43*, 911–920.
(8) Moon, Y.-A.; Shah, N. A.; Mohapatra, S.; Warrington, J. A.; Horton, J. D. Identification of a mammalian long chain fatty acyl elongase regulated by sterol regulatory element-binding proteins. *J. Biol. Chem.* **2001**, *276*, 45358–45366.
(9) Tvrdik, P.; Westerberg, R.; Silve, S.; Asadi, A.; Jakobsson, A.; Cannon, B.; Loison, G.; Jacobsson, A. Role of a new mammalian gene family in the biosynthesis of very long chain fatty acids and sphingolipids. *J. Cell. Biol.* **2000**, *149*, 707–718.
(10) Tvrdik, P.; Asadi, A.; Kozak, L. P.; Nedergaard, J.; Cannon, B.; Jacobsson, A. Cig30, a mouse member of a novel membrane protein gene family, is involved in the recruitment of brown adipose tissue. *J. Biol. Chem.* **1997**, *272*, 31738–31746.
(11) Zhang, K.; Kniazeva, M.; Han, M.; Li, W.; Yu, Z.; Yang, Z.; Li, Y.; Metzker, M. L.; Allikmets, R.; Zack, D. J.; Kakuk, L. E.; Lagali, P. S.; Wong, P. W.; MacDonald, I. M.; Sieving, P. A.; Figueroa, D. J.; Austin, C. P.; Gould, R. J.; Ayyagari, R.; Petrukhin, K. A 5-bp deletion in ELOVL4 is associated with two related forms of autosomal dominant macular dystrophy. *Nat. Genet.* **2001**, *27*, 89–93.
(12) Leonard, A. E.; Bobik, E. G.; Dorado, J.; Kroeger, P. E.; Chuang, L. T.; Thurmond, J. M.; Parker-Barnes, J. M.; Das, T.; Huang, Y. S.; Mukerji, P. Cloning of a human cDNA encoding a novel enzyme involved in the elongation of long-chain polyunsaturated fatty acids. *Biochem. J.* **2000**, *350*, 765–770.
(13) Jakobsson, A.; Westerberg, R.; Jacobsson, A. Fatty acid elongases in mammals: their regulation and roles in metabolism. *Prog. Lipid Res.* **2006**, *45*, 237–249.
(14) (a) Shimamura, K.; Kitazawa, H.; Miyamoto, Y.; Kanesaka, M.; Nagumo, A.; Yoshimoto, R.; Aragane, K.; Morita, N.; Ohe, T.; Takahashi, T.; Nagase, T.; Sato, N.; Tokita, S. 5,5-Dimethyl-3-(5-methyl-3-oxo-2-phenyl-2,3-dihydro-*1H*-pyrazol-4-yl)-1-phenyl-3-(trifluoromethyl)-3,5,6,7-tetrahydro-*1H*-indole-2,4-dione, a potent inhibitor for mammalian elongase of long-chain fatty acids family 6: examination of its potential utility as a pharmacological tool. *J. Pharmacol. Exp. Ther.* **2009**, *330*, 249–256. (b) Takahashi, T.; Nagase, T.; Sasaki, T.; Nagumo, A.; Shimamura, K.; Miyamoto, Y.; Kitazawa, H.; Kanesaka, M.; Yoshimoto, R.; Aragane, K.; Tokita, S.; Sato, N. Synthesis and evaluation of a novel indoledione class of long chain fatty acid elongase 6 (ELOVL6) inhibitors. *J. Med. Chem.* **2009**, *52*, 3142–3145. (c) Nagase, T.; Takahashi, T.; Sasaki, T.; Nagumo, A.; Shimamura, K.; Miyamoto, Y.; Kitazawa, H.; Kanesaka, M.; Yoshimoto, R.; Aragane, K.; Tokita, S.; Sato, N. Synthesis and biological evaluation of a novel 3-sulfonyl-8-azabicyclo[3.2.1]octane class of long chain fatty acid elongase 6 (ELOVL6) inhibitors. *J. Med. Chem.* **2009**, *52*, 4111−4114.
(15) Westerberg, R.; Mansson, J. E.; Golozoubova, V.; Shabalina, I. G.; Backlund, E. C.; Tvrdik, P.; Retterstol, K.; Capecchi, M. R.; Jacobsson, A. ELOVL3 is an important component for early onset of lipid recruitment in brown adipose tissue. *J. Biol. Chem.* **2006**, *281*, 4958–4968.
(16) Miyazaki, M.; Dobrzyn, A.; Man, W. C.; Chu, K.; Sampath, H.; Kim, H. J.; Ntambi, J. M. Stearoyl-CoA desaturase 1 gene expression is necessary for fructose-mediated induction of lipogenic gene expression by sterol regulatory element-binding protein-1c-dependent

and -independent mechanisms. *J. Biol. Chem.* **2004**, *279*, 25164–25171.
(17) Brolinson, A.; Fourcade, S.; Jakobsson, A.; Pujol, A.; Jacobsson, A. Steroid hormones control circadian Elovl3 expression in mouse liver. *Endocrinology* **2008**, *149*, 3158–3166.
(18) Kumadaki, S.; Matsuzaka, T.; Kato, T.; Yahagi, N.; Yamamoto, T.; Okada, S.; Kobayashi, K.; Takahashi, A.; Yatoh, S.; Suzuki, H.; Yamada, N.; Shimano, H. Mouse Elovl-6 promoter is an SREBP target. *Biochem. Biophys. Res. Commun.* **2008**, *368*, 261–266.
(19) Jakobsson, A.; Jorgensen, J. A.; Jacobsson, A. Differential regulation of fatty acid elongation enzymes in brown adipocytes implies a unique role for Elovl3 during increased fatty acid oxidation. *Am. J. Physiol.* **2005**, *289*, E517–E526.
(20) Jorgensen, J. A.; Zadravec, D.; Jacobsson, A. Norepinephrine and rosiglitazone synergistically induce Elovl3 expression in brown adipocytes. *Am. J. Physiol.* **2007**, *293*, E1159–E1168.
(21) Westerberg, R.; Tvrdik, P.; Unden, A. B.; Mansson, J. E.; Norlen, L.; Jakobsson, A.; Holleran, W. H.; Elias, P. M.; Asadi, A.; Flodby, P.; Toftgard, R.; Capecchi, M. R.; Jacobsson, A. Role for ELOVL3 and fatty acid chain length in development of hair and skin function. *J. Biol. Chem.* **2004**, *279*, 5621–5629.
(22) Shimamura, K.; Miyamoto, Y.; Kobayashi, T.; Kotani, H.; Tokita, S. Establishment of a high throughput assay for long chain fatty acyl-CoA elongase using homogeneous scintillation proximity assay. *Assay Drug Dev. Technol.* **2009**, in press.
(23) Lilian, A. R.; Young, S. L.; James, R. M.; Michael, E. P. Synthesis of HIV-1 reverse transcriptase inhibitor DMP 266. *Synth. Commun.* **1997**, *27*, 4373–4384.
(24) Miwa, H.; Hiyama, C.; Yamamoto, M. High-performance liquid chromatography of short-and long-chain fatty acids as 2-nitrophenylhydrazides. *J. Chromatogr. A* **1985**, *321*, 165–174.